Processing & Characterization of PZT Thin Films Through Sol-Gel Process

By

Farhan Javaid

Supervisors

Dr. Amir Azam Khan
Dr. Asghari Maqsood

Submitted to the Department of Materials Engineering (SCME), in partial fulfillment of requirements for the degree of Masters in Materials and Surface Engineering.

National University of Sciences and Technology
School of Chemical & Material Engineering
Islamabad, Pakistan.

June, 2009

This research work is dedicated

To

my beloved parents and teachers who have the great wish for my success in life and helped me in every manner in the completion of such a higher level of education beyond their limits

Abstract

The present work is based upon processing & characterization of Lead Zirconate Titanate powder / thin films through sol-gel process. Lead acetate tri-hydrate, zirconium n-propoxide and titanium iso-propoxide are used as source precursors for lead, zirconium & titanium respectively. Initially, a blackish powder is obtained after drying the mixture of the three precursors at 300^{o}C for one hour. Further heat treatment at 600^{o}C resulted in a yellowish powder, a usual color for perovskite powder after calcination. The PZT powders hence obtained are characterized through XRD and SEM analysis. XRD results show a presence of PZT phase after calcination at 600 ºC for one hour and a particle size calculated using scherrer's equation of approx: 28 nm. In addition, single & double layer Lead Zirconate Titanate thin films are coated on silicon and brass (70:30) substrates by using sol-gel dip coating process at 600^{o}C. Surface topography, morphology and micro-structures of PZT coated films are investigated using contact mode Atomic Force Microscopy (AFM) and Scanning Electron Microscope (SEM). The AFM & SEM analysis provides evidence that the PZT thin films coated on silicon and brass (70:30) substrates are uniform and dense, with signs of shrinkage associated with the removal of volatile species during treatment at high temperature. Initial experiments are also conducted to produce the PZT coating by using sol-gel spin coating process. These coatings are produced on 70:30 Brass disk. SEM analysis endow with evident that homogeneous PZT thin film attain as a result of spin coating process.

ACKNOWLEDGEMENTS

First of all I would like to thank Allah Almighty for enabling me to take on this project with success which is also the last milestone of M.Sc. degree course. Nothing could have been possible without His guidance.

Secondly, I offer my most sincere gratitude to my project supervisor Dr. Amir Azam Khan for his guidance & support throughout of my stay in the university; especially giving his precious time for extensive discussion & always encouraging me in developing critical thinking in this project. In addition my thanks also go to my co-supervisor Dr. Asghari Maqsood for her kind supervision & guidance in interpreting XRD results.

Great thanks to Mr. Khalid Rao for providing me help regarding PZT Sol and giving a broad vision of PZT synthesis technique. Without his co-operation fissure of my project were hard to fill.

I would also like to thank the faculty of SCME, especially to Dr. K.Sana who allowed me to use labs facility even in university closing hours, Dr Muhammad Islam for superb AFM Images and Dr. Mujahid for SEM study of PZT thin film cross-sections.

And at the last, my special thanks to all of my class mates for supporting me throughout my master's degree, especially to Mr. Arshad Bashir who helped me in XRD analysis, Mr Tauheed Shahbaz for wonderful SEM micrographs, Mr. Jibran & Mr. Junaid for practical work support.

Table of Contents

1

Introduction

Ceramics are inorganic materials that consist of metallic and non-metallic elements chemically bonded together [1]. This term appeared at Dolni Vestonice (in the former Czechoslovakia), as early as 24,000 BC [2]. Since then, ceramics are being used in various applications. But the ceramic materials used in engineering applications, can be divided into two groups: Traditional ceramic (made from three basic components clay, silica & feldspar) and Engineering ceramics (consists of pure or nearly pure compound). Due to attractive characteristics such as high hardness, wear resistant, chemical stability, high temperature strength, low co-efficient of thermal expansion, higher value of piezo-electricity etc. advance ceramics selected for a hefty applications.

Among these applications, ceramic as piezoelectric materials are widely used in even many critical area like electro-optic devices, non-volatile memories, actuators etc. In piezoelectric materials, electric charge is generated on application of force, or conversely the deformation of the material when a potential is applied (phenomenon known as piezoelectric effect). Its more detail is briefly discussed in chapter 2.

Present work is based upon processing & characterization of thin film coating of a well known piezoelectric material Lead Zirconate Titanate, which is one of the extensively used piezoelectric compounds of engineering ceramics. It is also known as PZT which is an abbreviation of its chemical formula (Pb Zr_x Ti_{1-x} O_3). PZT is widely known for its high dielectric and piezoelectric properties. The same is use in the form of powders, fibers or as thin/thick coating on variety of substrates (Metallic, non-metallic, semi-conductor etc). Thus enable PZT to use in large variety of

applications such as ferro-electric nonvolatile memories, transducers, sensors, capacitors, switches etc. Chapter 2 will give a brief picture of lead Zirconate Titanate.

In earlier work [3] conducted at SCME, the strontium doped PZT was prepared using conventional sintering techniques. This technique can be divided into five stages: powder mixing, drying, calcination, shaping and sintering. The main difficulty at some stage in this technique is the high volatility of lead oxide (PbO) due to its lower melting point i.e. 886^{o}C. In conventional sintering technique, PZT perovskite phase appear during calcination, which is carried out in range of temperature very close to the melting point of PbO. Thus, there are probabilities of loss of lead oxide during calcination and sintering [4,5,6].

In order to retain as much PbO as possible, calcination / sintering may be performed with the component surrounded by lead-rich powder such as lead zirconate and enclosed in a lidded crucible. Even with these precautions, there is usually a slight loss of PbO occurs, causes a slight deficiency of lead in final product, which adversely affects the piezo-electric properties [7, 8]. In order to compensate the loss of lead oxide, addition of excess quantity of the same in the start of batch is widely used by several authors [9,10].

In contrast, some of the workers suggested that excess of lead should be avoided in perovskite materials; because the excess PbO either precipitate at the grain boundaries[11], damaging the electrical properties, or shift the PZT composition toward the titanium lean side, since TiO_2 has higher solubility then zirconia in the lead oxide liquid phase. In addition, lead is toxic and exposure to lead compounds has a cumulative effect. It is therefore necessary that evaporation is controlled.

In the light of above, some low temperature processing techniques are key constraint where homogeneous compositions products are required. Sol-gel processes provide the alternate route for low temperature processing of PZT.

In the past decades, extensive research and development have resulted in increased awareness of the sol-gel process. As the name indicates, sol-gel process consists of two steps. First we form a sol (a suspension of colloidal particles or molecules in a liquid or solution) and in second step this sol is converted into gel. In ceramic synthesis, two different routes have been identified and depend on the gel structure.

- **Particulate Gel (**Using a network of colloidal particles**)**
- **Polymeric Gel (**Using an array of polymeric chains**)**

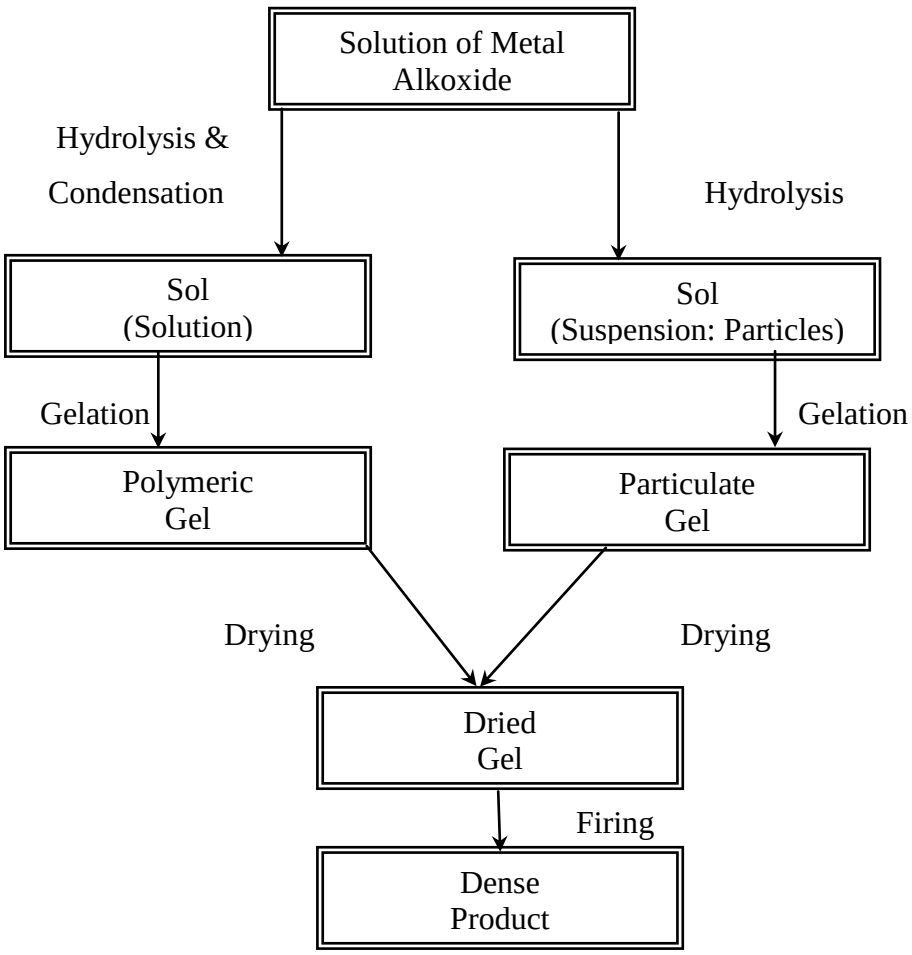

Fig. 1.1: *Flow chart comparison of sol-gel process using solution and suspension of fine particles*

The process that occur depends upon the form of the sol, i.e., whether it is a solution or a suspension of fine particles. Flow diagram (Fig. 1.1) clearly indicates the difference between both of the process. In the present work, we are mainly concerned with the polymeric gel route.

Sol-gel processing is versatile because it can be used to produce ceramics in a number of different forms:

- ***Powders:*** because we can make very small particles & control the composition.

- ***Coatings:*** because the sol is a viscous liquid and can be applied to substrate via dipping, spinning and spraying techniques.

- ***Fibers:*** because we can pull a thread out that is liquid and dries it, coat it, etc.

- ***Crystalline or Glass:*** We have the choice, e.g., High - purity porous glass for filtration.

In the present work, we are mainly concerned with powder and thin films synthesis. Powders can be obtained via sol-gel process using metal alkoxides or combination of metal alkoxides. Because the mixing of the constituents is achieved at a molecular level, the powder is chemically homogeneous, acquire high surface area, allowing them to be sintered to nearly full density at desired temperatures as compared to the preparation been made by other techniques.

Ceramic coatings can be prepared by using a sol-gel process involving metal alkoxides. The coating may be formed by dipping, spinning, spraying, flow coating and lowering (similar to dipping except the substrate remains stationary and the liquid is lowered). These coating techniques are widely used to produce thin films of PZT for micro-electronic systems. Further detail on sol gel process and sol-gel coatings are briefly discussed in chapter 3 and 4.

The gel obtained during sol-gel synthesis, usually consists of weak skeleton of amorphous material containing an interconnected network of small liquid-filled pores. The liquid is usually a mixture of alcohol and water, which must be removed. There are several different methods used to dry gels. Table 1.1 provides a brief description of these different methods.

Table 1.1: *Different types of dry gels*

Types	***Drying Conditions***	***Micro-structure***
Aerogels	In an autoclave, the fluid is removed by hypercritical evacuation.	A network consisting of ~95% porosity.
Xerogels	Natural evaporation	Dried gel has about 40–60% of the fired density and contains small pores (as small as 2 nm)
Sonogels	Gel exposed to ultrasound in the 20-kHz range prior to autoclave treatment.	Assists in the formation of multi-component gels
Cryogels	Freeze dried	Finely divided powder, not suitable for producing monolithic ceramics

Different characterization techniques can be use to follow the transitions that occur during sol-gel processing. There are two parts of the process in which we are interested:

i. *The transition from sol to gel.*

ii. *The transition from gel to oxide.*

Few techniques used to characterize the sol-gel process and type of information they can provide is listed in Table 1.2.

Table 1.2: *Characterization techniques employed for sol-gel process*

Technique	*What is measured*	*How it is used*
DTA	Phase Transformation, Enthalpy change	Phase transition during gelation, drying
SEM	Crystallinity & Phase identification, micro-structure at high resolution	Transformation from amorphous to crystalline during firing; experiment can be formed in situ
X-ray diffraction	Crystallinity & Phase identification	Transformation from amorphous to crystalline during firing; experiment can be formed in situ
FTIR	Qualitative & quantitative identification of functional group.	Chemical changes during gelation, drying and firing.
Raman spectroscopy	Compound identification, Structural order & phase change.	-do-

2

Perovskite Structures, PZT and Their Applications

The present work is based upon the synthesis & characterization of thin film ceramic known as *lead zirconate titanate (PZT)*, which belong to a class of ceramic called "Perovskite". Before going through the detail, familiarity of following few terms are obligatory [12]:

2.1 ***Piezoelectric Effect:***

It may be defined as, "A Process in which electric charge is generated by certain materials on application of force, or conversely the deformation of the material when a potential is applied."

2.2 ***Ferroelectric Effect:***

The ferroelectric effect is an electrical phenomenon whereby certain crystals may exhibit a spontaneous dipole moment.

2.2.1 ***Difference between piezoelectric & Ferroelectric effect:***

There are a lot of fundamental differences between the piezoelectric & ferroelectric effect. But the most important practical difference lies in mathematical relationship between the stress (or strain) and the electric field. In a piezoelectric material this relationship is linear i.e.

Piezoelectric change in thickness = dE

Whereas for the ferroelectric effect is quadratic i.e.

Ferroelectric change in thickness = dE^2

Where d is the piezoelectric charge constant and E is the applied emf.

2.3 ***Piezoelectric Properties:***

2.3.1 ***Piezoelectric Charge Constant (d):***

The *piezoelectric charge constant*, d, is the polarization generated per unit of mechanical stress applied to a piezoelectric material or, alternatively, is the mechanical strain experienced by a piezoelectric material per unit of electric field applied.

2.3.2 ***Mechanical Quality Factor:***

It may be define as "ratio of energy supplied per cycle to energy dissipated per cycle".

2.3.3 ***Electromechanical coupling coefficient (k):***

The electromechanical coefficient, k, is a measure of the efficiency of the piezoelectric material to convert one form of energy into other form.. It is given by the Eq.

$$k^2 = \frac{\textit{Mechanical energy converted into electrical charge}}{\textit{Mechanical energy put into piezoelectric material}}$$

Or

$$k^2 = \frac{\textit{Electrical energy converted into Mechanical charge}}{\textit{Electrical energy put into piezoelectric material}}$$

"k" is quite often expressed as a percentage. Thus, a material for which k value approaches 1 (100%) is best at converting the energy from one form to the other.

2.3.4 ***Dielectric Loss Factor:***

It is the measure of electric energy lost (as heat energy) by a piezoelectric material in ac circuit.

2.3.5 ***Poling:***

A process in which ferro-electric materials can be transformed into polar materials by applying a static field.

Poling is necessary only for ferroelectric materials but not for inherently piezoelectric materials in single crystal form. The piezoelectric change in thickness can be positive or negative whereas the ferroelectric change in thickness can only be positive. Because of this, the application of a sinusoidal emf to a piezoelectric material results in a strain which is sinusoidal.

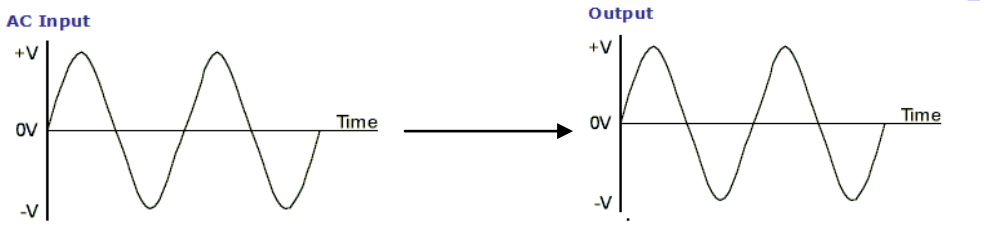

Sinusoidal emf Input Piezoelectric material output

Fig. 2.1(a): *Piezoelectric Material response*

In contrast, if the same thing is done to ferroelectric material, the resulting strain is in fact, a rectified but unsmoothed sinusoidal curve.

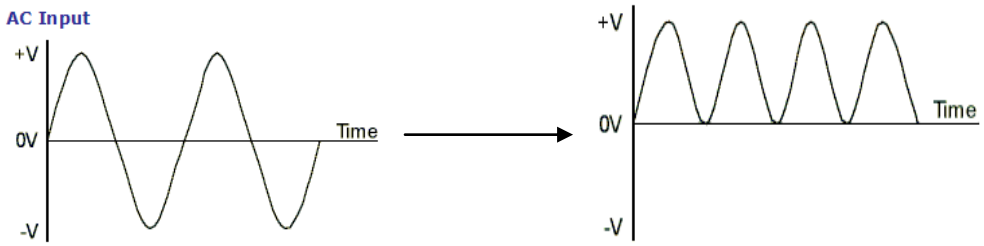

Sinusoidal emf Input Ferroelectric material output

Fig. 2.1(b): *Ferroelectric Material response*

Thus the trick to obtain a resultant sinusoidal stain curve is hidden in poling.

2.4 ***What are Perovskites?***

The mineral $CaTiO_3$ was discovered in the Ural Mountains by geologist G. Rose in 1839 and given the name perovskite in honor of the eminent Russian mineralogist, Count Lev Alexevich von Perovski [13]. The name perovskite is now used to refer to any member of a very large family of ceramics that has the formula ABO_3 and for which the *B* ion is surrounded by an octahedron of *Oxygen* ions. A simple perovskite structure is shown in fig. 2.2.

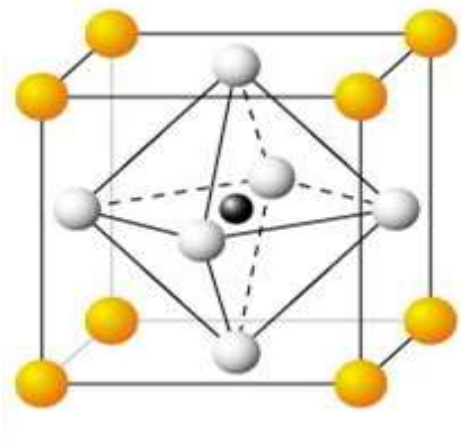

Fig. 2.2: *Perovskite structure*

The perovskite oxides are extremely interesting because of the enormous variety of solid-state phenomena they exhibit. These materials include insulators, piezo-electric, semiconductors, metals, and superconductors. Some have delocalized energy-band states, some have localized electrons, and others display transitions between these two types of behavior. Many of the perovskites are magnetically ordered and a large variety of magnetic structures can be found.

Scientific studies of the perovskites date back many years [2]. The physical properties of the tungsten bronzes were investigated as early as 1823 [13]. However, it is only in recent years that experimental and theoretical information on the electronic structure has begun to become available. Energy band calculations, neutron diffraction and inelastic scattering data , photoemission spectra , optical spectra, and

transport data are now available for materials such as ReO_3, WO_3, $NaWO_3$, $SrTiO_3$, $BaTiO_3$, $KMoO_3$, $KTaO_3$, $LaMnO_3$, $LaCoO_3$, PZT and a variety of other perovskites.

2.5 ***An Introduction to PZT:***

Lead Zirconate Titanate also known as PZT which is an abbreviation of its chemical formula (Pb Zr_x Ti_{1-x} O_3) belongs to a class of ceramic perovskites. Discovery of PZT as a piezo-electric material in 1950s was a major breakthrough in the research of piezo-electric materials [14]. A unit cell of PZT is shown in figure 2.3.

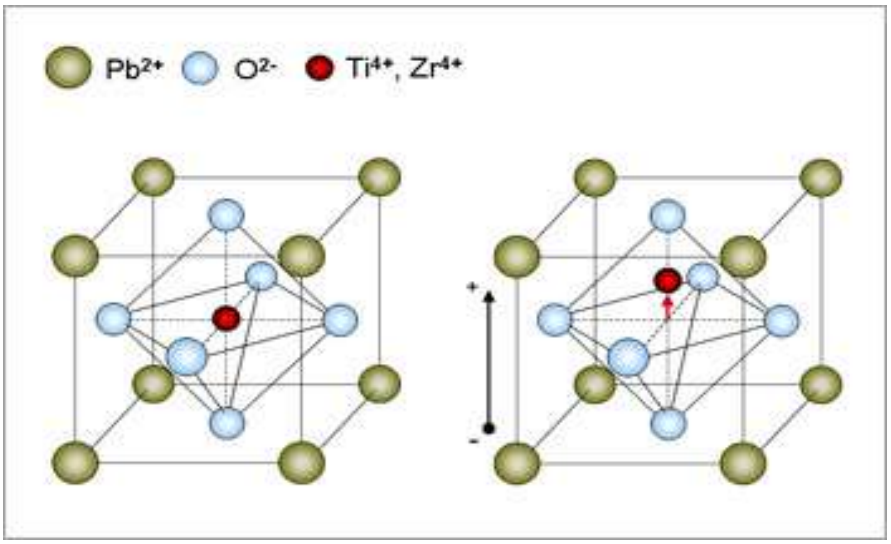

Fig. 2.3: *A PZT unit cell*

This ceramic of perovskite family exhibited very high piezo-electric & dielectric properties. Furthermore, PZT offered the possibility of tailoring their behavior to specific response and applications by the use of Dopants. To date, PZT is one of the most widely used piezoelectric materials.

The ions lie at the corners of the unit cell are termed as A site and in PZT that are occupied by Pb^{+2} ions and the ion which lie at interstices in oxygen octahedra are called B site. Zr or Ti ion fills this space in PZT. The arrangement of cations and anions is such that cations are shielded from one another by oxygen ions. Each oxygen ion (in face position in unit cell) is coordinated by four Pb (at the corners of unit cell) and two Ti or Zr ion [15]. Interstitial space in oxygen octahedra is larger than

the size of B cation so that it can rattle around in the space and may go close to any oxygen ion when acquire stable position.

2.6 ***Lead Zirconate Titanate (PZT) Phase Diagram***:

Lead Zirconate Titanate (PZT) is a binary solid solution of $PbZrO_3$ an anti-ferroelectric (orthorhombic structure) and $PbTiO_3$ a ferroelectric (tetragonal perovskite structure). The PZT phase diagram is shown in Fig. 2.4.

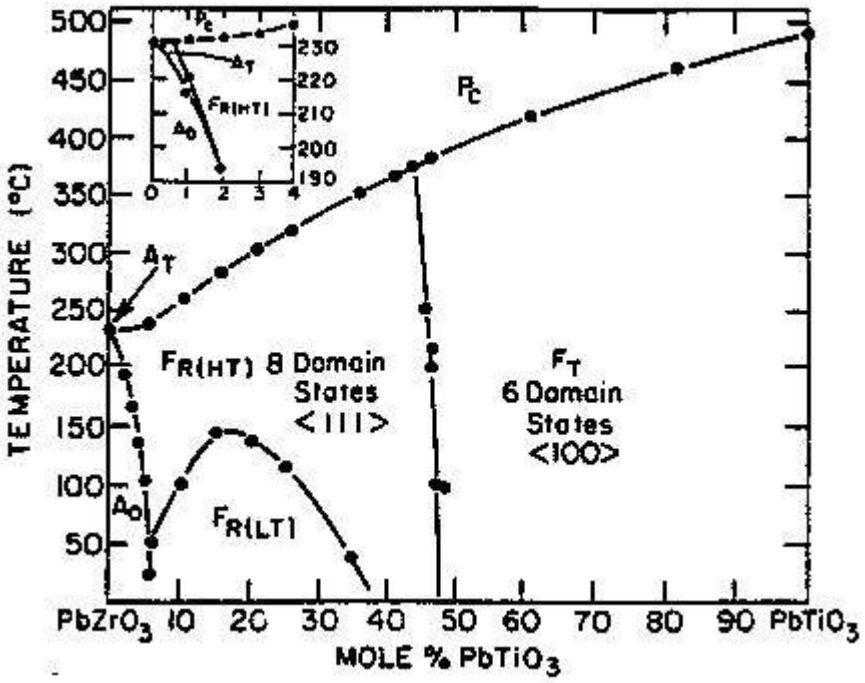

Fig. 2.4 : *The PZT phase diagram.* [16]

At high temperatures PZT has the cubic perovskite structure which is para-electric. On cooling below the Curie point line, the structure undergoes a phase transition to form a ferroelectric tetragonal or rhombohedral phase. In the tetragonal phase, the spontaneous polarization is along the <100> set of directions while in the rhombohedral phase the polarization is along the <111> set of directions. A significant feature of the phase diagram of figure 2.4 is the presence of the morphotropic phase boundary (MPB). The MPB denotes an abrupt structural change with composition at constant temperature in the solid solution range. The MBP composition range has believed to be quite narrow, but in practice the MPB has a wide range of compositions over which the tetragonal and rhombohedral phases

coexist in ceramics [17,18,19]. Both the dielectric constant and the piezoelectric coefficients near the MPB are enhanced due to the meta-stable co-existence of tetragonal and rhombohedral phases resulting in a maximum poling efficiency and electromechanical activity.

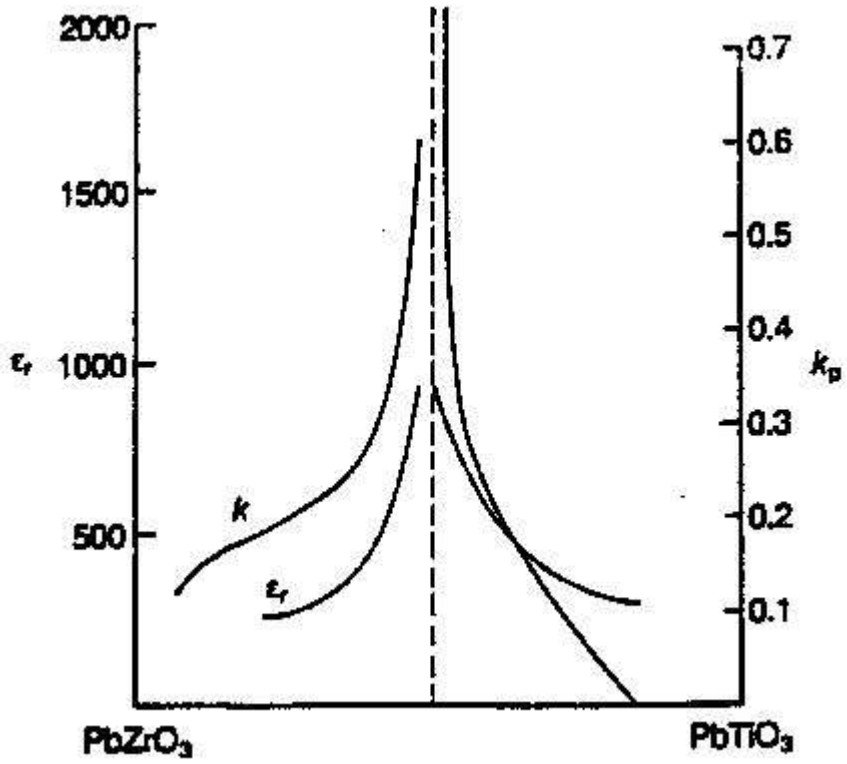

Fig. 2.5: *shows that most physical properties such as dielectric and piezoelectric constants show an anomalous behavior at the morphotropic phase boundary (MPB)*

The MPB separating the two ferroelectric tetragonal and orthorhombic phases has a room temperature composition with a Zr/Ti ratio of ~ 52/48. PZT ceramics with the MPB composition show excellent piezoelectric properties.

The coexistence of two phases over a range of compositions close to the MPB was demonstrated by S. Zhao *et al* [17]. The lattice parameters of the tetragonal structure of $Pb(Zr_{1-x}Ti_x)O_3$ films are changed as a function of the titanium content x. It was observed that the c/a lattice ratio decreased as the Ti content x increased [20].

The poling of the PZT ceramic is also easy at MPB composition because the spontaneous polarization within each grain can be switched to one of the 14 possible orientations (eight [111] directions for the rhombohedral phase and six [100] directions for the tetragonal phase). Below the Zr/Ti ratio of 95/5 the solid solution is anti-ferroelectric with an orthorhombic phase. On the application of an electric field to this composition a double hysteresis loop is obtained. This is because of the strong influence of the anti-ferroelectric $PbZrO_3$ phase.

2.7 ***Effect of Dopants on PZT properties:***

In order to suit some specific requirements for certain applications, piezoelectric ceramics can be modified by doping them with ions which have a valence different than the ions in the lattice. Piezoelectric PZT ceramics having the composition at the MPB can be doped with ions to form "hard" and "soft" PZT's.

2.7.1 ***Hard PZT's:***

Hard PZT's are doped with acceptor ions such as K^+, Na^+ (for A site) and Fe^{3+}, Al^{3+}, Mn^{3+} (for B site), creating oxygen vacancies in the lattice. Hard PZT's usually have lower permittivities, smaller electrical losses and lower piezoelectric coefficients. These are more difficult to pole and de-pole, thus making them ideal for rugged applications.

2.7.2 ***Soft PZT's:***

On the other hand, soft PZT's are doped with donor ions such as La^{3+} (for A site) and Nb^{5+}, Sb^{5+} (for B site) leading to the creation of A site vacancies in the lattice [21]. The soft PZT's have a higher permittivity, larger losses, higher piezoelectric coefficient and are easy to pole and de-pole. They can be used for applications requiring very high piezoelectric properties.

2.8 ***Application of PZT:***

The number of applications of PZT grew very rapidly with the development and improvement of lead zirconate titanate based components. A comprehensive description of all applications is practically impossible. However, few applications are appended below:

- ✓ Ferro-electric Memories
- ✓ Transducers
- ✓ Sensors
- ✓ Capacitors
- ✓ As a switch
- ✓ Ultra-sonic imaging
- ✓ Optical filters
- ✓ Shutters
- ✓ Actuators

3

Sol-Gel Process

Brinker and Scherer [22] define sol-gel as:

"The preparation of ceramic materials by preparation of a sol, gelation of the sol, and removal of the solvent"

The process starts by making a solution known as sol which is colloidal suspension of particles in liquid with suitable reagents. One of the basic components of the sol is the precursor which carries the metal atom desired in the end product. This solution will gelate under certain conditions to form one large polymeric molecule with liquid captured inside resulting product known as gel [22].

Sol to gel formation is just one part of ceramic synthesis via sol-gel process. The second part involves the heat treatment of the gel including drying, ageing, calcination, sintering etc. Depending upon the application this gel can be heat treated in order to obtain powders, thin films, fiber, monoliths or aerogel.

The concept of sol-gel process used to obtain different products is illustrated in figure 3.1.

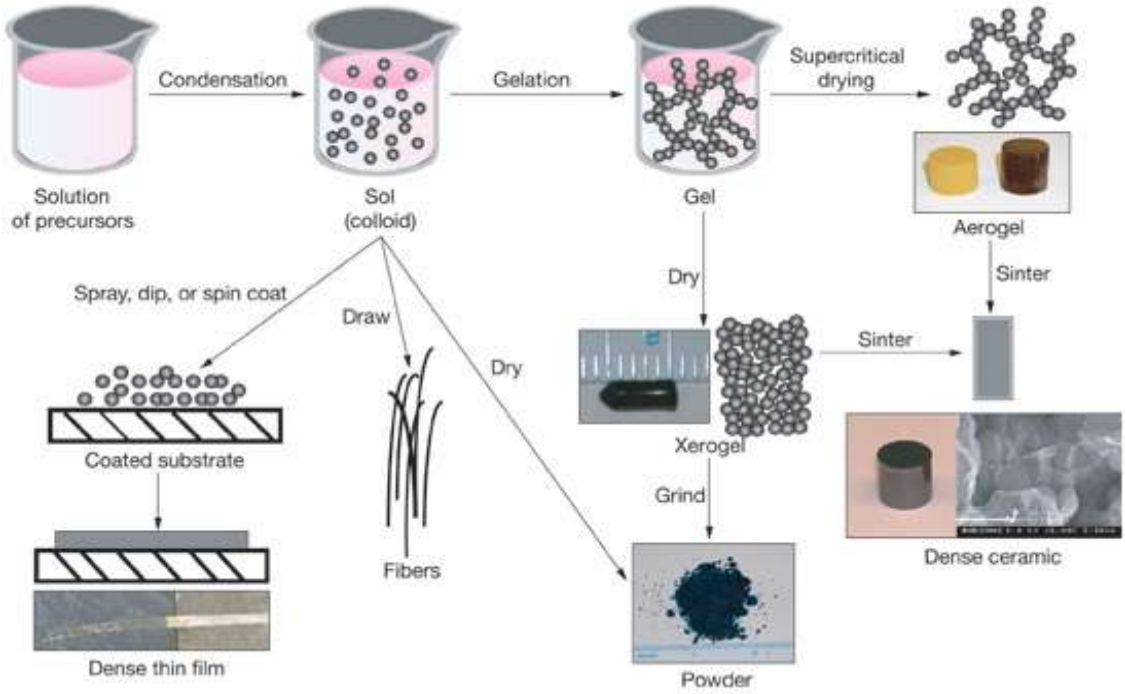

Fig. 3.1: *Different product route using sol-gel process*

3.1 ***History of Sol-Gel Process:***

The French chemist J.J. Ebelman was the first to synthesize a metal alkoxide i,e tetra-ethoxysilane (TEOS) in 1840s by treating $SiCl_4$ with ethanol [22]. The resulting clear liquid had a tendency of becoming a gel under atmospheric conditions. He was succeeded in gelation of TEOS accidentally due to presence of moisture in air. In absence of air, its gelation is impractically slow (months). Eblemen was known to be interested in ceramics and mineralogy. However, he did not further develop the idea of forming ceramics in low temperatures through the sol-gel process, and the invention of sol-gel process faded into oblivion for the decades.

In 1930s, German glass manufacturer Schott and Genossen[23], coated optical oxide films by sol-gel process, so first commercially interesting application were found. But unfortunately, Schott's process did not use precursors latter commonly used i.e. TEOS and it is possible that the process was too slow to be practice.

After the Second World War, sol-gel technology found some niches, such as preparation of homogeneous powders in ceramics and even in nuclear industry[24]. In 1970s, Yoldas[25] and some other researchers published results on possibility of producing monoliths by sol-gel process. The development of sol-gel technology has been rapid during the last few decades [24].

3.2 ***Basic Chemistry of Sol-Gel Process:***

The sol - gel process is typically based on the use of alkoxide starting reagents and alcohol solvents [22,26,27]. Metal alkoxides, M(OR)n, are the derivatives of alcohols, ROH, which are usually easily accessible, extremely weak as acids, easily removable via hydrolysis and thermal treatment, leaving high purity hydrated oxides . This makes metal alkoxides the most common candidates for sol-gel process precursors.

Depending on the material system and starting reagent reactivity, relatively common alcohols, such as methanol and ethanol, may be used as solvents. However, for more reactive alkoxide starting reagents, less common alcohols such as 2 - methoxyethanol and 1–3 propanediol have also found widespread utilization. Two main reactions involve during the sol-gel processing are

(i). Hydrolysis
(ii). Poly-Condensation.

Considerations in selection of reagent(s) and solvent are to exert control over the hydrolysis and condensation reactions that lead to oligomerization, i.e., the development of short polymeric species. The first part of the process is hydrolysis, a reaction between the metal alkoxide and water. In this reaction water molecules replace the alkoxy groups with hydroxide groups. The result is a metal hydroxide and alcohol.

Hydrolysis:

$$M(OR)_x + H_2O \longrightarrow M(OR)_{x-1}(OH) + ROH \quad \text{…….(Eq. 3.1)}$$

The metal hydroxides will react with each other and with free alkoxide groups. In this reaction water is released, the result is an oxide link between the two metal molecules i,e M-O-M plus the released water molecule. This part of the process is called poly condensation.

Condensation (water elimination)

$$2M(OR)_{x-1}(OH) \longrightarrow M_2O(OR)_{2x-2} + H_2O \quad \text{……..(Eq. 3.2)}$$

Condensation (alcohol elimination)

$$2M(OR)_{x-1}(OH) \longrightarrow M_2O(OR)_{2x-3} + ROH \quad \text{…….(Eq. 3.3)}$$

These reactions have been studied in detail for materials such as silica, and understanding of reaction mechanisms, as well as of the role of the precursor and catalyst (acid or base), has been well documented [28]. Similar studies have been carried out in other material systems, most notably, Lead Zirconate Titanate [$Pb(Zr,Ti)O_3$; PZT] [29-30].

It is important to understand that these two processes, hydrolysis and poly-condensation, are accompanied with a physical process, drying. When the polymer has been formed, it is in the form of a gel, a large single molecule with a continuous liquid phase in the molecule. In the macroscopic world this could be analogous to a sponge. During the drying process the solvents evaporate from the gel, and a solid polymer is formed.

3.3 ***Gelation:***

The reactions (Eq. 3.1 – Eq. 3.3) lead to the growth of clusters, until they begin to impinge on one another and gelation occurs by a linking of these clusters through percolation process. Near the gel point, bonds form at random between the nearby clusters, linking them into a network. The gel point corresponds to the percolation threshold, when a single cluster (called the spanning cluster) appears. The spanning clusters co-exist with sol containing many small clusters, which gradually become attached to the network. It reaches across the vessel that contains it so the sol doesn't pour when the vessel is tipped. By creating a continuous solid network, the

spanning cluster is responsible for abrupt rise in the viscosity and appearance of an elastic response to stress.

The theories can be divided into three main classes: classical theory, percolation theory, and kinetic models. *Classical theory* is based on the theory of Flory and Stockmeyer[22]. The classical theory provides a good description of the gel point; however, it provides an unrealistic description of polymer growth in sol–gel silicates. *Percolation theory* [22] avoids the unrealistic assumptions of the classical theory and makes predictions of the gelling systems that are in good accord with experimental observations. A disadvantage is that only a few results can be obtained analytically, suggesting that these models must be studied by computer simulations.

The *kinetic models* are based on Smoluchowski's analysis of cluster growth. The geometry of the clusters is not considered specifically in the theory, but the size distribution and shape of the clusters determined by computer simulation are in good agreement with experiment. The predictions of polymer growth and fractal structure are also in good agreement with experimental observations. The growing clusters eventually overlap and become immobile, so that further bonding involves a percolation process. The evolution of the properties in the vicinity of the gel point is generally in agreement with the critical behavior predicted by percolation theory.

3.4 ***Aging of Gels:***

Aging in sol gels is defined as the collection of processes which take place between gelation and the point at which the final materials can be processed. The four processes most recognizable during the aging period are

- Poly-condensation
- Syneresis
- Coarsening
- Phase transformation

3.4.1 ***Polycondensation:***

Poly-condensation or condensation was mentioned in the early sections and need not be discussed further except to say that the condensation reaction rate can be increased by applying heat.

3.4.2 ***Syneresis:***

As the condensation reaction proceeds, new bonds are formed bridging neighboring chains, causing the network to contract. As the network contracts the solvent trapped in the pores is forced out. This simultaneous contraction of the network and expulsion of solvent is called *Syneresis*. Several factors can affect Syneresis. This whole process occurs in an aqueous system and the ability of two species to join together and undergo a condensation reaction is a function of electrostatic van-der-Waals forces. The extent of condensation and shrinkage can therefore be controlled by addition of electrolytes. Heat can also increase shrinkage to the extent that heat increases the rate of condensation.

3.4.3 ***Coarsening:***

Third main process come into play during aging of gel is *coarsening*. Coarsening is the "growth" of larger particles of a substance from smaller particles. An example of the process of coarsening would be to partially melt fine-grained sand in a crucible. As the melt cools, larger particles form and the overall texture are coarser. In the case of the sol-gel, smaller particles dissolve in the available solvent and re-precipitate in the cracks between neighboring larger particles. This re-precipitation has the result of filling in the smaller pores and shifting the statistical distribution of pore size to larger volumes. Particle centers do not migrate and thus the degree of shrinkage is unaffected.

3.4.4 ***Phase Transformation:***

Solid-liquid, liquid-liquid, and solid-solid phase transformations are possible in the gel during the drying process. An example of a solid-liquid phase transformation is micro-syneresis in which the polymer chains show a greater attraction to other chains than for the solvent in which they are growing. Rather

than branching out into the solvent, the chain "clump" together and result is the production of gel pores with a great volume.

Liquid- liquid phase transformations, as expected, occur between two liquids which can phase separate and are usually not readily miscible with each other. A good example is the base-catalyzed hydrolysis of silicon alkoxides. When soaked in pure water, the gel turns white which is attributable to droplets of partially hydrolyzed alkoxide. Finally, there are the solid-solid phase transformations where materials that were initially amorphous become, at least partially, crystalline. The overall process is very similar to coarsening with the same factors that affect the rates.

3.5 ***Drying:***

To obtain the final product the solvent has to be removed from the gel. The simplest method, referred as conventional drying, is to remove the solvent by evaporation in air or in a drying chamber such as oven. The gel produced by conventional drying is referred as *xerogel*. If the gel is dried by removal of solvent under supercritical conditions, the gel is referred as *aerogel*. In this case, no shrinkage occurs, so gel is highly porous (e.g., typically 90-95% porosity in polymeric gels).The rate of removing the solvents affects the physical properties of the end product very significantly. The drying process can be divided into two major stages:

a. A constant rate period (CRP) where the evaporation rate is nearly constant
b. A falling rate period (FRP) where the evaporation rate decreases with time or the amount of liquid remaining in the body.

The stages of drying process are shown graphically figure 3.2:

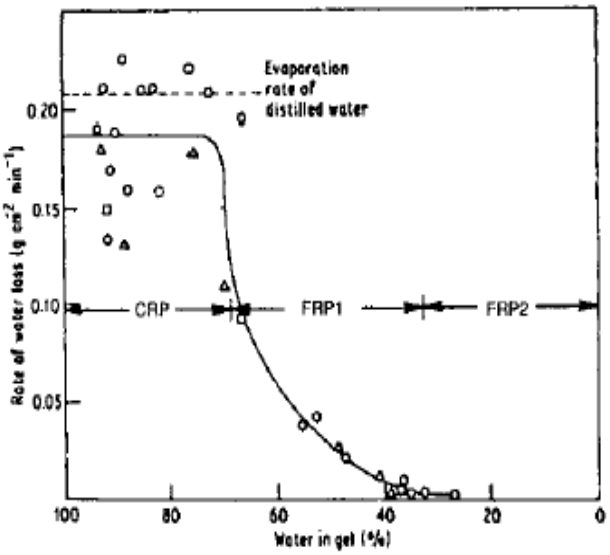

Fig. 3.2: *Different stages of drying*

In constant rate period, the rate of evaporation is constant. When evaporation starts, the temperature at the surface of gel drops, because of loss of heat due to latent heat of vaporization of liquid. However, heat flow to the surface from the atmosphere quickly establishes thermal equilibrium where transfer of heat to the surface balances the heat loss due to the latent heat of vaporization.

When the shrinkage stops, further evaporation forces the liquid meniscus into the pores, and the evaporation rate decreases. This stage is referred as *Falling rate Period.* In some materials it is possible to further separate the FRP into two parts. In the first falling rate period (FRP1), the evaporation rate decreases approximately linearly with time, while in the second falling rate period (FRP2), the rate decreases in a curvilinear manner as shown in figure 3.2.

3.6 ***Calcination:***

Calcination is a thermal treatment process in which a substance is heated to a high temperature (but blow the melting point), in order to bring about a thermal decomposition, phase transition or removal of a volatile fraction.

In general, term calcination is widely used in industrial processes i.e. calcination of limestone, petroleum coke etc. The same is used extensively in ceramic

processing especially in processing of ceramics through *conventional oxide technique* and *sol-gel process*. In both of aforesaid ceramic processing techniques, calcination is carried out in order to obtain a phase change or related processes (decomposition, volatilization of solvents etc). For example, in case of PZT synthesis via sol-gel process, dried gel is calcined to obtain a crystalline PZT structure. But key of success is hidden in the selection of calcination temperature and soaking time. These two factors decide the final properties of ceramics.

Calcination is carried out in furnace or kiln (of various designs including shaft furnaces, rotary kilns, multiple hearth furnaces etc.) under vacuum / air or control atmospheres depending upon sensitivity / application of final product.

3.7 ***Advantages & Limitation Of Sol-Gel Process:***

3.7.1 ***Advantages:***

i. High purity
ii. Low temperature processing
iii. High chemical homogeneity with multi-components
iv. Preparation of ceramics and glasses with novel composition.
v. Ease of fabrication for special products such as films, fibers etc.

3.7.2 ***Limitation:***

i. Expensive raw material
ii. Large shrinkage during fabrication
iii. Drying step lead to long fabrication time.
iv. Limited to fabrication of small articles.
v. Special handling of raw material usually required.

3.8 ***Application of Sol-Gel Process:***

Applications of sol-gel process in different fields are given in table below:

Application	***Composition***	***Products***
Abrasives	Alumina + dopants	Cutting tools, Abrasive grains
Aerogels	Silica, titania	Thermal & Acoustic Insulator
Membranes	Alumina, Titania, Zirconia	Nano filters, ultra-filters
Nuclear	UO_2, ThO_2 micro-spheres	Nuclear fuel for fission reactor
Fibers	Al_2O_3-ZrO_2-SiO_2	Reinforcement
Fibers	Al_2O_3-ZrO_2-SiO_2	Reinforcement
Optics	SiO_2	Lens
Electronics	PZT, PLZT	Piezo-electric & Optical coatings
Coatings	Zirconia, SiO_2-Na_2O-B_2O_3	Corrosion barrier To concentrate laser beams in nuclear reactor
Thin Films	TiO_2	Interference Filters

4

Sol-Gel Coating Techniques

One of the key features of sol-gel process is the manufacturing of thin films on different substrates (metallic & non-metallic). This can be achieved prior to gelation of sol. Most commonly technique uses for sol-gel ceramic coating on different substrates are:

- Dip Coating
- Spin Coating
- Spraying
- Flow Coating

4.1 ***Dip Coating:***

In dip coating process, the object to be coated is lowered into the solution and withdrawn at a suitable speed. In practice, dip coating is currently the more widely used. For dip coating, the contact angle between the sol and the surface of the object should be low so that the sol wets and spreads over the surface.

Dip coating can be performed employing either continuous or batch processing. Scriven[31] divided the batch dip coating into five stages: immersion, start up, deposition, drainage, and evaporation as shown in figure 4.1.

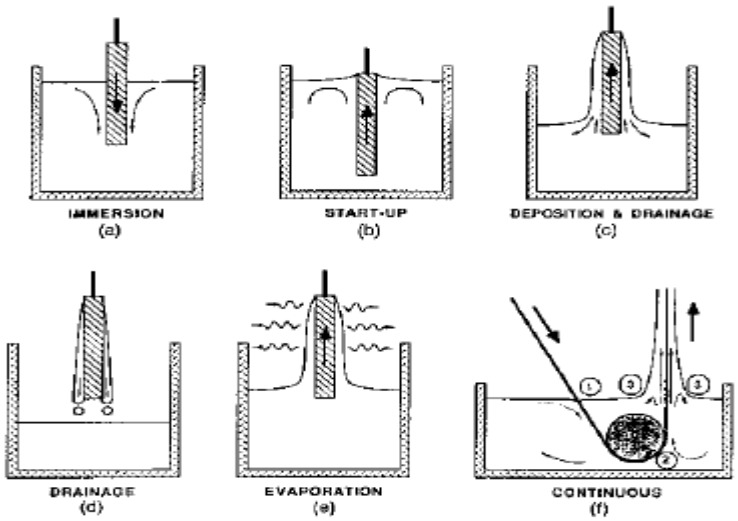

Fig. 4.1: *Showing different stages of batch type process and continuous dip coating process* [31]

The continuous dip coating process is simple as it separates immersion from the other stages essentially eliminates start up, hides drainage in deposition of film and restrict the evaporation to the deposition stage and afterwards.

The thickness of film mainly affected by following forces:

1. Viscous drag upward on the liquid by the moving substrate
2. Force of gravity
3. Resultant force of surface tension in the concavely curved meniscus,
4. Inertial force of the boundary layer liquid arriving at the deposition region
5. Surface tension gradient

In addition, according to Brinker and Hurd [32], the thickness of the film formed is determined by the viscosity (ŋ), and density (ρ) of the sol and withdrawal speed or rate (U).

$$t = 0.94\frac{(\eta U)^{2/3}}{\gamma^{1/6}(\rho g)^{1/2}}$$

Where γ and g are the surface tension and acceleration caused by gravity.

This equation clearly indicates that thickness of film (t) is directly proportional to viscosity (ŋ) and withdrawal speed (U). So by increasing the ŋ of the sol and withdrawal rate of substrate thickness of film can increase. Advantages & limitation of dip coating are appended below:

4.1.1 ***Advantages:***

- Very simple process
- Thickness from 20nm to 50µm can be obtained.
- Irregular shapes can be coated
- Can be a continuous process
- Economical process

4.1.2 ***Limitations:***

- Thickness variation
- Voids and pin holes due to entrapment of air, surface contamination, or dust particles
- Not suitable for curved surfaces
- Difficult to save one side of substrate.

4.2 ***Spin Coating:***

In spin coating process, the sol is dropped onto the object, which is spinning at a high speed. Scravin [31] divided the spin coating process into four stages: deposition, spin-up, spin off, and evaporations shown in figure 4.2. In spin-up stage, liquid flows radially outward, driven by the centrifugal forces generated by the rotating substrate, leaving as droplets. As the film gets thinner, the rate of removal of excess liquid by spin off become slower because of greater resistance to flow and greater effect of evaporation in raising the viscosity by concentrating the non-volatile component of the solution. In forth stage, evaporation becomes primary mechanism of thinning.

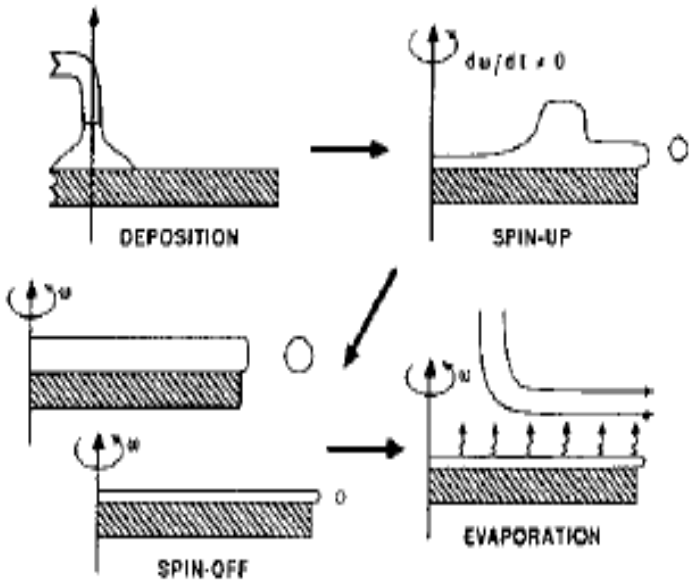

Fig. 4.2: *Stages of spin coating process* [31]

The coating sol / solution are dispensed on the substrate either manually or by an automatic robotic arm. This substrate is then accelerated to a very high angular velocities *(~300 to 10,000rpm)* during which the excess liquid is spun off from the substrate leaving a thin uniform film. Thickness less then 30nm to a few microns per layer can easily achieve.

Basic concept behind the spin coating involves the equilibrium between the centrifugal forces created by the rapid spinning and the viscous forces determined by the viscosity of the sol [33-34]. The film thickness can be varied by controlling

(a) Spin Speed
(b) Time
(c) Viscosity of sol

It has been observe that [33], the film thickness (t) is inversely proportional to square root of angular velocity. So, this coating technique has been used to deposit ultra-thin (10nm) to thick (5µm) coatings on flat substrates depending upon the angular velocity of rotating substrate, viscosity of sol and time provided for whole process.

Advantages & Limitations of spin coating techniques are appended below:

4.2.1 ***Advantages:***

- Excellent control over thickness.
- Reproducibility
- Various materials, including resin, epoxy, and polymers can be successfully coated on metal, glass, ceramics, plastics, papers, and semiconductors substrates.
- Spin coating leads to coating of one side of the object only.

4.2.2 ***Limitations:***

- Because of spinning, large objects coating is impractical.
- The objects to be coated are commonly in the shape of small, flat disks.
- Large material loss

4.3 ***Spray Coating:***

In spray coating process, very fine droplets are formed from the coating solution using atomizers or nebulizers [33] as shown in Fig. 4.3

Fig. 4.3: *Spray coating process* [35]

Compared with dip & spin coating, the sol viscosity has to be greatly reduced to facilitate the nebulization process to form fine droplets.

These fine droplets are then carried into the coating chamber with a carrier gas and deposited on the substrate by gravity or with an electrostatic field, where the negatively charged droplets are attracted to the electrically grounded substrate. The advantages of electrostatic spray coating over traditional gravitational spray coating are high deposition rates and low material loss. Materials savings of 25% to 50% over traditional spraying techniques have been reported [36].

The spray - coating technique are widely used in industry mainly for its ability to coat non-planar structures like steps, trenches, and stacks on semiconductor chips [36]. Philips has developed a combined spin and spray process for functional sol-gel coatings on TV screens. Advantages and limitations of spray coating are given below:

4.3.1 ***Advantages:***

- High Efficiency
- Fast & adaptable to complex shapes and sizes

4.3.2 ***Limitations:***

- Expensive process
- Low viscosity sol required.
- Wastage of sol material

4.4 ***Flow Coating Process:***

In flow coating process, the liquid is poured over the substrate to be coated as shown in fig.4.4.

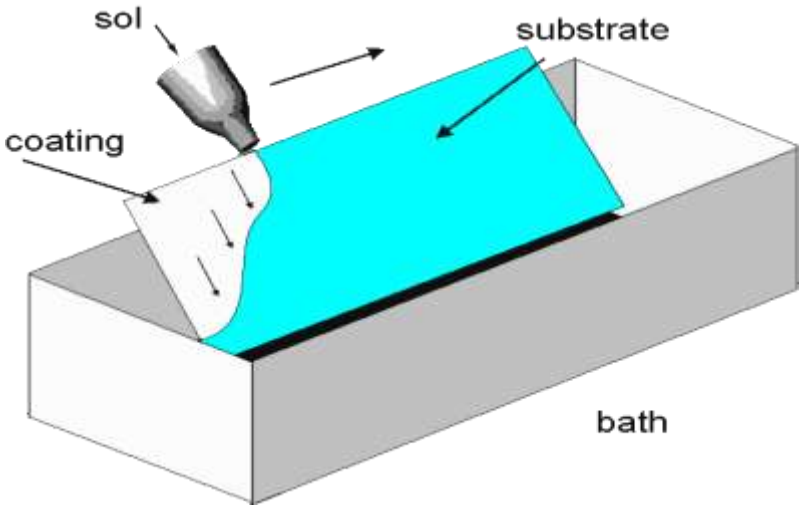

Fig. 4.4: *Sol-Gel flow coating process*

Factors affecting the thickness of film are

- Inclination of substrate
- Sol viscosity
- Solvent evaporation rate

Main advantage of flow coating process is that, the non-planer large substrates can be coated rather easily.

4.5 ***Film Formation:***

Film formation characteristics strongly affected by [37-39]:

i. The precursor use.
ii. Phase segregation
iii. Tendencies toward de-wetting
iv. Surface morphology of substrate.
v. Solvent

Solvent itself don't take a part in chemical reaction but during thin film coating, an improper choice of solvent can causes phase separation [37]. Significant work has been carried out to prepare films that range in thickness from tens of nanometers [38] to 10μm[39]. Short - chain alcohols are commonly used as solvents for the former, whereas diol compounds, such as 1,3 - propanediol [40-41] have been used to fabricate thicker layers. The short – chain alcohols have higher vapor pressures, which lead to capillary forces that can drive precursor species into greater proximity during film drying and thus lead to a chemical reaction between the precursor species. This behavior can lead to a film that possesses a higher crosslink density (between precursor species) and that may be more resistant to densification caused by the presence of M - O - M bonds. In contrast, low volatility solvents can inhibit reactivity between precursor species. This may lead to de-wetting of the substrate. Solution concentration and viscosity represent additional important factors in film processing. The greatest impact of these properties is on film thickness. Typically for sol - gel processed films, striations are readily apparent to the naked eye as film non-uniformities.

4.6 ***Heat Treatment Effect on films:***

After film formation, the films are subjected to a heat treatment process for removal of residual organic species (entrapped solvent as well as the organic constituents associated with the precursor species), densification (elimination of residual porosity and structural free volume in the film), and crystallization.

From a practical perspective, the organic removal step is typically carried out at temperatures of between 200 ° C and 400 ° C [33]. Densification and crystallization have been carried out using box or tube furnaces, although rapid thermal annealing has also been used in many instances. Heat treatment schedules that use a single thermal process also been employed successfully by some workers [33-41]. Typical physical processes that occur after film deposition and associated temperature ranges are shown in Fig. 4.5.

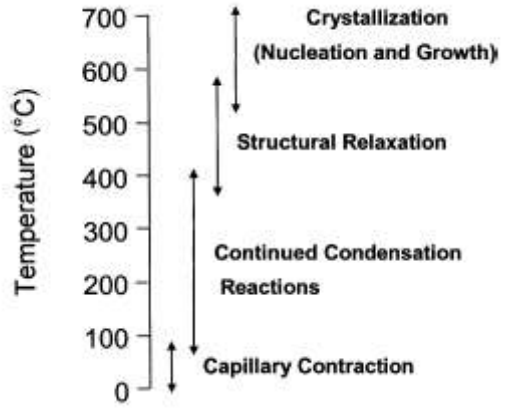

Fig. 4.5: *Approx. temperature ranges for heat treatment of thin films.*

As solvent is removed from the film (which may begin during the spin - off stage of the deposition process and continue during drying, and then during low - temperature heat treatment), fine - scale (nm size) porosity may be created. At the interface with the solvent remaining in the pores, significant pressures can develop. These pressures contribute to capillary contraction, which can be a substantial driving force for the structural collapse of the film, which leads to densification. As the film collapses, reactive groups on different precursor molecules within the film come into closer proximity, which causes additional condensation reactions. This densification mechanism is accelerated as temperature is increased and organic groups from the precursor species are removed. Once the bulk of the organic materials have been removed from the film, other characteristics of the film will be altered, including the structural free volume associated with the inorganic amorphous state [42-43]. This "structural relaxation" leads to continued densification of the film. Finally, for crystalline materials such as high permittivity dielectrics and ferroelectric materials, crystallization occurs via a nucleation and growth process [44,45,46].

Computational techniques can be used to probe crystallization behavior. Dobberstein and his coworkers [47] developed a pixel - by - pixel approach to study the transformation behavior of a lead zirconate titanate thin film using an approach based on classic nucleation theory, the kinetic rate of crystal growth and bulk material properties. To simplify the simulation, crystallographic orientation was restricted to three principal directions: <100>, <110>, and <111>.

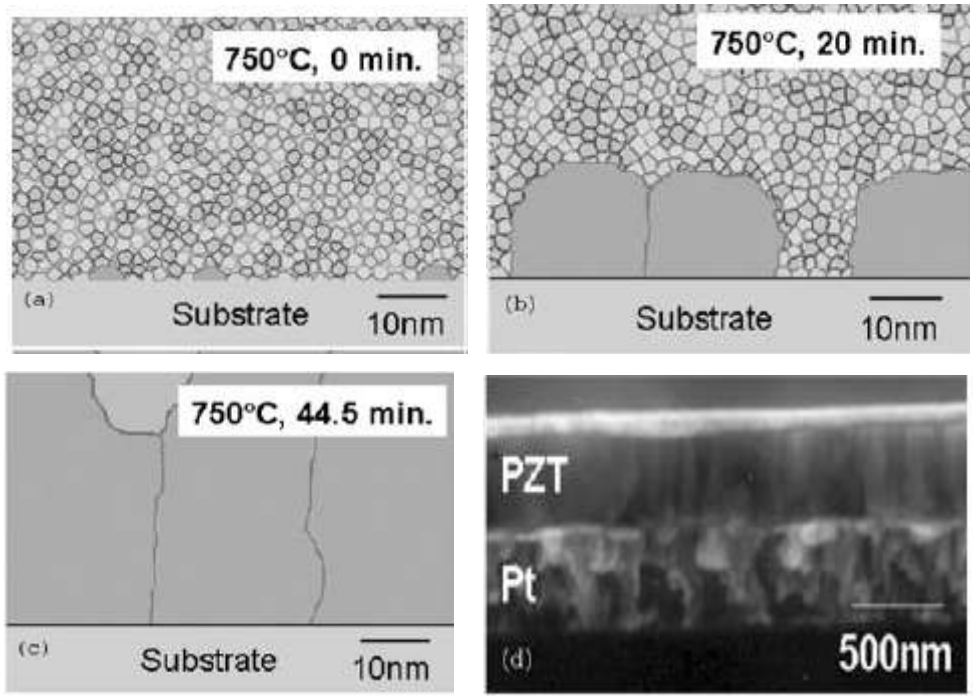

Fig. 4.6: (a-c) *Simulation of film structural evolution for PZT thin films at various times during heat treatment* ***(d)*** *a representative SEM photograph illustrating the columnar micro-structure of PZT.*

This simulation "snapshots" clearly indicate that, at 750^{o}C nucleation and growth increases with soaking time and at the end columnar micro-structure is predicted (Fig. 4.6(a) to4.6(c)). For comparison, a CSD - prepared PZT thin film microstructure is shown in Fig. 4.6(d). Although the predicted and actual grain sizes are different by approximately a factor of five; but general aspects of the microstructure are effectively captured. In the future, the use of such methods might facilitate an improved understanding of the role of processing conditions on thin film microstructure.

5

Experimental Procedure

5.1 ***Sol Preparation:***

For present research, PZT sol of composition according to formula ***Pb (Zr $_{0.52}$ Ti $_{0.48}$)*** O_3 were obtained as per recipe given in following flow sheet diagram.

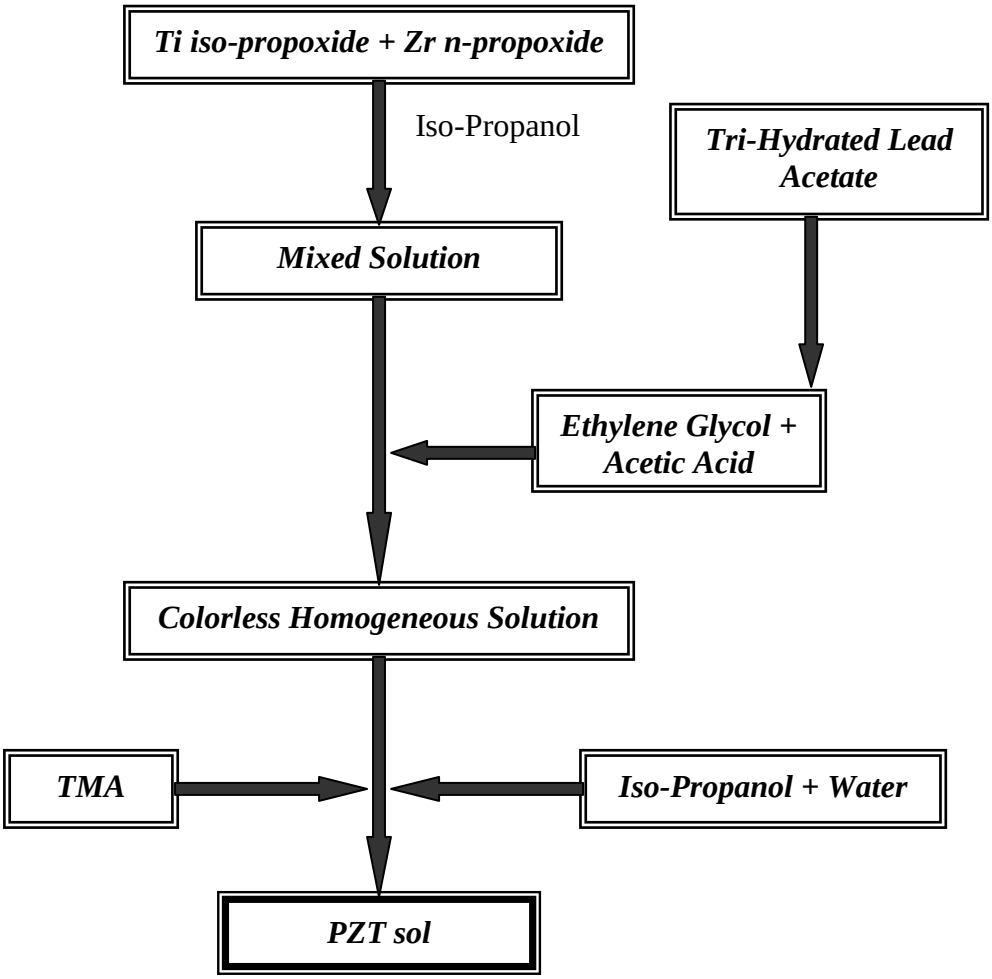

Fig. 5.1: *PZT Sol Synthesis Flow Sheet Diagram*

Precursors *lead acetate tri-hydrate, zirconium n-propoxide* and *titanium iso-propoxide* were used as source for lead, zirconium & titanium respectively. Iso-propanol and Ethylene glycol were used as solvents resulting 300ml of PZT sol as per recipe given in figure 5.1. PZT sol hoard in a refrigerator in order to prolong the storage time. This composition is selected due to fact that, by the side of this, one can attain better piezo-electric properties. The experimental procedures adapted for present work are appended below.

5.2 ***Sol's pH Measurement:***

First of all pH of the sol was measured using pH meter. For this purpose, pH meter was calibrated to 7.0. Then sol was taken in a beaker and in order to report a precise result, average of pH readings calculated i.e. 6.45.

5.3 ***PZT Powder Preparation:***

Two powder samples were prepared from PZT sol through sol-gel process. Description of these powder samples are given in Table 5.1.

Table 5.1: *Powder Samples ID & Description*

Sr. #	***Sample ID***	***Description***
1	*PZT – I*	*Black color powder obtained after drying the dark brown gel at 300^{o}C*
2	*PZT – II*	*Light yellow color PZT powder obtained after calcination of black Powder at 600^{o}C*

5.3.1 ***Preparation of Calcined Light Yellow Color Powder:***

To prepare powder sample PZT – II, 10ml of PZT sol was taken in a 50ml beaker. Then, the same beaker placed in oven at 120^{o}C for 24 hours results dark brown gel. After that, this gel left at 120^{o}C for three days in order to obtain dried

powder but no powder was formed. So the sample was heated at 300^{o}C for one hour. This turned out into black swollen mass. Later, this black swollen PZT precursor mass was grounded to a fine powder and calcined at 600^{o}C for one hour. After calcination, color of powder changed to light yellow. Then the sample was preserved in air tight bottle for characterization i.e. XRD and SEM analysis.

5.3.2 ***Preparation of Dried Black Color Powder:***

To prepare powder sample # PZT – I, 10ml of PZT sol was taken in a test tube. In contrast to sample PZT – II, sol was heated at 120^{o}C for 30minutes and gradually shrinkage rate was observed until the shrinkage at macro-level bunged.

Then the sol was left in an oven for conversion into dark brown gel. For substantiation of the process done in preparation of sample PZT – II, gel was again kept at 120^{o}C for three days in an oven but the results were same as obtained against sample PZT – II i.e. no gel to powder conversion crop up. So, again the gel was heated to 300^{o}C in an oven for one hour that result a swollen black mass which was grounded to obtain fine powder. Resultant sample was preserved for characterization i.e. XRD & SEM analysis

5.4 ***Sol-Gel Dip Coated Samples:***

Four samples of PZT thin film were prepared by using sol-gel dip coating process on silicon and brass (70:30) substrates. Details of four samples are described in Table 5.2.

Table 5.2: *PZT Coated Samples ID & Description*

Sr. #	***Sample ID***	***Description***
1	*Si – LT*	*PZT coated sample on silicon wafer at Low temperature (300^{o}C)*
2	*Si – HT*	*PZT coated sample on silicon wafer at High temperature (600^{o}C)*
3	*B – LT*	*PZT coated sample on brass at Low temperature (300^{o}C)*
4	*B – HT*	*PZT coated sample on brass at High temperature (600^{o}C)*

5.4.1 ***Preparation of Sol-Gel Dip Coated Samples:***

Details regarding the preparation of sol-gel dip coated samples are appended below:

5.4.1.1 ***PZT Coated Brass Samples Preparation:***

PZT coated brass samples were prepared as per sequence shown in figure 5.2.

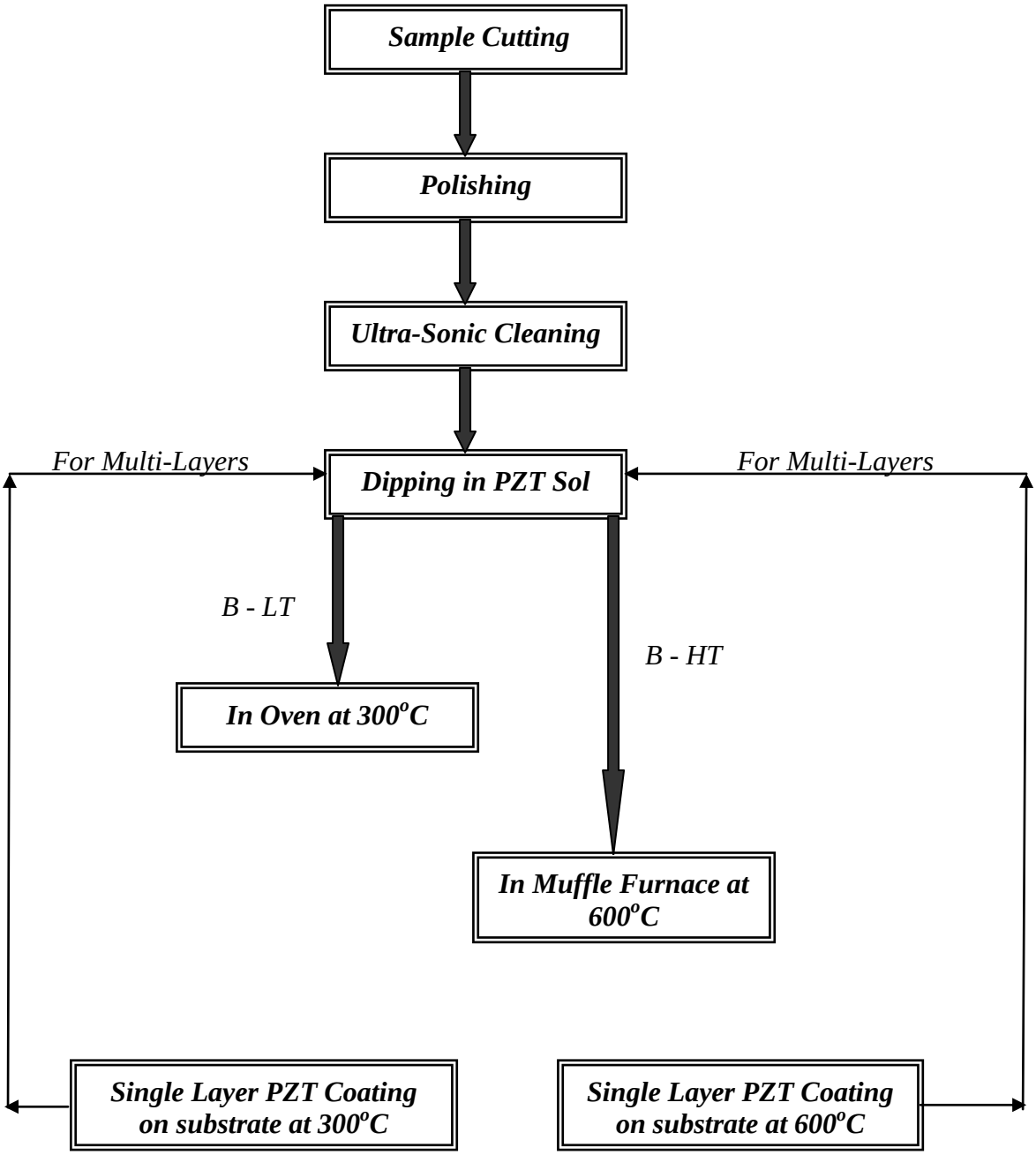

Figure 5.2: *PZT Sol – Gel Dip Coating Process Sequence*

Initially, both brass samples were cut to size and polished up to 800 micron emery paper. Cleaning of samples was carried out through ultra-sonic cleaning in ethanol for 10 minutes. Then, both samples were dip in PZT Sol and after withdrawal with constant speed, sample B – LT was kept at 300^{o}C for one hour and sample B – HT kept at 600^{o}C for 10 minutes. To obtain multi-layers, repeated coating procedure is adopted as shown in figure 5.2. These samples were preserved for further characterization i.e. AFM & SEM analysis.

5.4.1.2 ***PZT Coated Silicon Samples Preparation:***

Two PZT coated silicon samples i.e. Si – LT and Si - HT were prepared in same manner as PZT coated Brass samples, with elimination of just IInd step (Fig. 5.2). Both of samples were then preserved for further characterization i.e. AFM and SEM analysis.

5.5 ***Sol-Gel Spin Coated Samples:***

Sample B-5 was prepared via sol-gel spin coating process. Brass (70:30) disc polished on polishing wheel up to 800 microns emery paper. After polishing, brass disc was cleaned for 10 minutes in ethanol using ultrasonic cleaning. Finally took 2ml of PZT sol in a dropper & introduced the same (drop by drop) on brass disc rotating at speed 300rpm. Meanwhile, the rotation speed of sample was increased gradually up to 400rpm. Whole exercise took 10 minutes. The brass coated PZT sample was heated for 10 mins at 600^{o}C in a pre-heated Muffle furnace and allowed to cool in the same furnace. Then the PZT coated brass disc was preserved for further SEM analysis.

6

Results & Discussion

Earlier chapter provides a brief picture of project experimental sequence. This chapter will endow a comprehensive discussion on the observations made during experimental work.

6.1 ***Powder Samples:***

In the preparation of powder sample PZT – I, initially a noticeable shrinkage during sol to gel conversion were observed. After first 30 minutes when the sol was kept at 120^{o}C, ~60% shrinkage (of the total quantity of sol) occurs. During next two hours more shrinkage appeared, but not as sharp as observed in first 30 minutes. After four hours, the shrinkage at macro-level bunged and viscosity of the sol increased.

This shrinkage occurs due to the evaporation of the low volatile solvents from the sol. Low volatile solvents evaporate continuously and volume of the sol goes on decreasing until evaporation of such solvents (like alcohols) was completed.

Hyun Tae Lee [48] used the same precursors as in present work. Lee [48] kept the gel at 100^{o}C for three days and successfully obtained dark reddish brown PZT powder. Same soaking time & 120^{o}C temperature was applied for sample PZT - II in the present work but results were diverse than the results of Hyun Tae Lee [48].

In present work, after three days, more viscous dark brown gel was obtained. During preparation of sample PZT – I, same thing was verified by keeping the sol at 120^{o}C in an oven for three days but results were same i.e. no PZT powder was formed. While going through the literature review, the disparity between present and Hyun Tae Lee [1] work can be explained as following.

In present work acetic acid was used in the preparation of the sol that created the chelating effect. During hydrolysis, the acetate group of acetic acid bonded with the titanium atom and consequently hindered the gel formation and prolongs the drying stage. Chemical reaction for the same is appended below:

$$M(OR)_4 + xCH_3COOH \longrightarrow M(OR)_{3-x}(OOCCH_3)x + xROH$$

The acetate groups can be removed efficiently only when the heating temperature is higher than 300^{o}C [49]. According to Merkle's investigation [50], several intermediate reactions occur during the decomposition of the lead acetate. These multiple reactions are shown as the following:

$$Pb(CH_3COO)_2 \xrightarrow{220^{o}C - 270^{o}C} Pb(CH_3COO)_2 . PbO \quad \ldots\ldots\ldots \text{(Eq. 6.1)}$$

$$\xrightarrow{270^{o}C - 310^{o}C} Pb(CH_3COO)_2 . 2PbO \quad \ldots\ldots\ldots \text{(Eq. 6.2)}$$

$$\xrightarrow{310^{o}C - 350^{o}C} PbO_{1-x}(CO_3)_x \quad \ldots\ldots\ldots \text{(Eq. 6.3)}$$

$$\xrightarrow{350^{o}C - 415^{o}C} PbO \quad \ldots\ldots\ldots \text{(Eq. 6.4)}$$

Thus keeping in view the above literature study, both samples were kept at 300^{o}C for 1 hour in an oven and this time results were satisfactory i.e., Black PZT powder obtained as shown in figure 6.1.

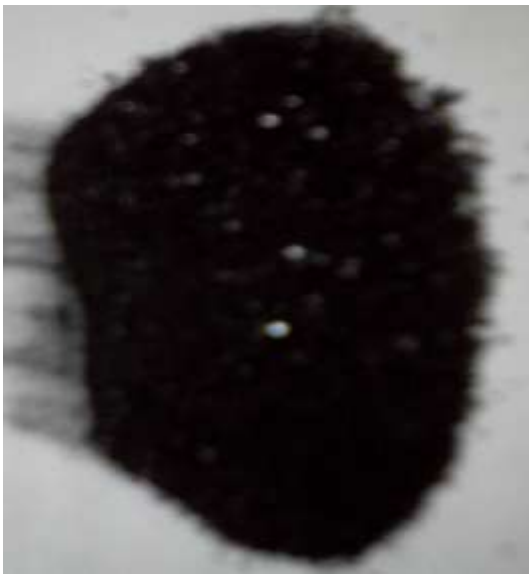

Fig. 6.1: *Dried black powder obtained at 300^{o}C*

Powder obtained in sample PZT – II was subjected to calcination at 600^{o}C in a muffle furnace for one hour and the outcome was a light yellow PZT powder as shown in figure 6.2.

Fig. 6.2: *Calcined light yellow powder obtained at 600^{o}C*

The structure of powders PZT – I dried at 300^{o}C & PZT – II calcined at 600^{o}C were studied by X-ray diffraction (Cu Kα radiations). The XRD pattern of the PZT – I is shown in fig. 6.3.

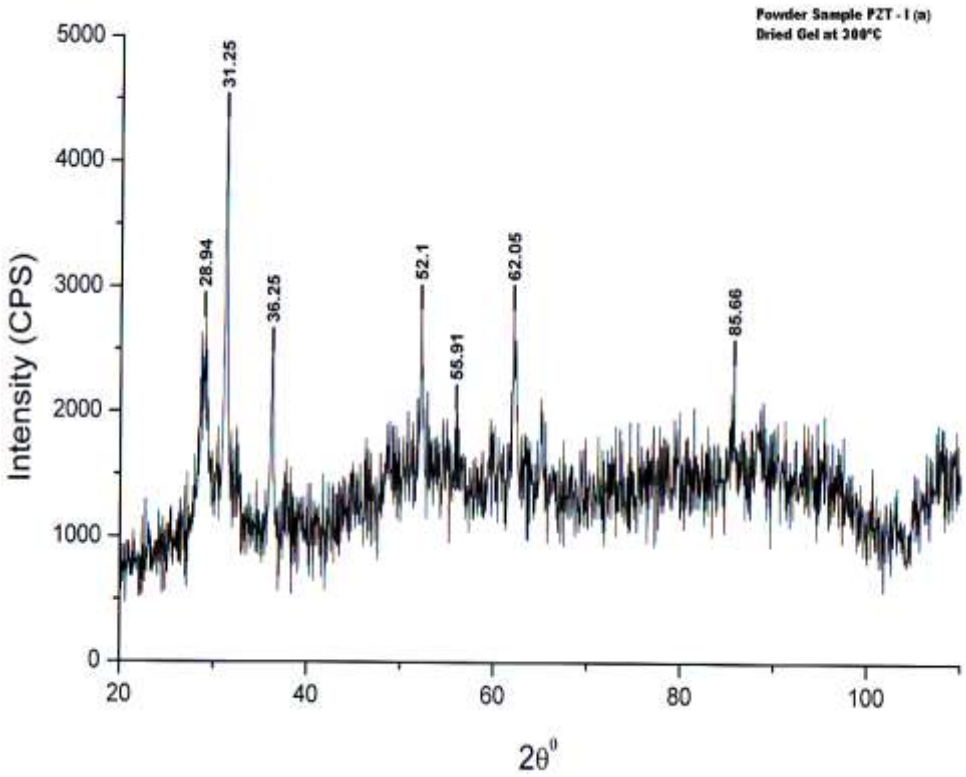

Fig. 6.3: *XRD Pattern of PZT – I Powder Dried at 300^{o}C*

PZT – I XRD pattern point out that the dominant phase at 300^{o}C was the Lead Oxide. The XRD results were in good agreement with the decomposition reactions of anhydrous lead acetate to the lead oxide phase given in Eqs. 6.1 to 6.4.

By increasing the temperature, PbO phase begins to vanish and PZT phase appear in the XRD (Fig. 6.4).

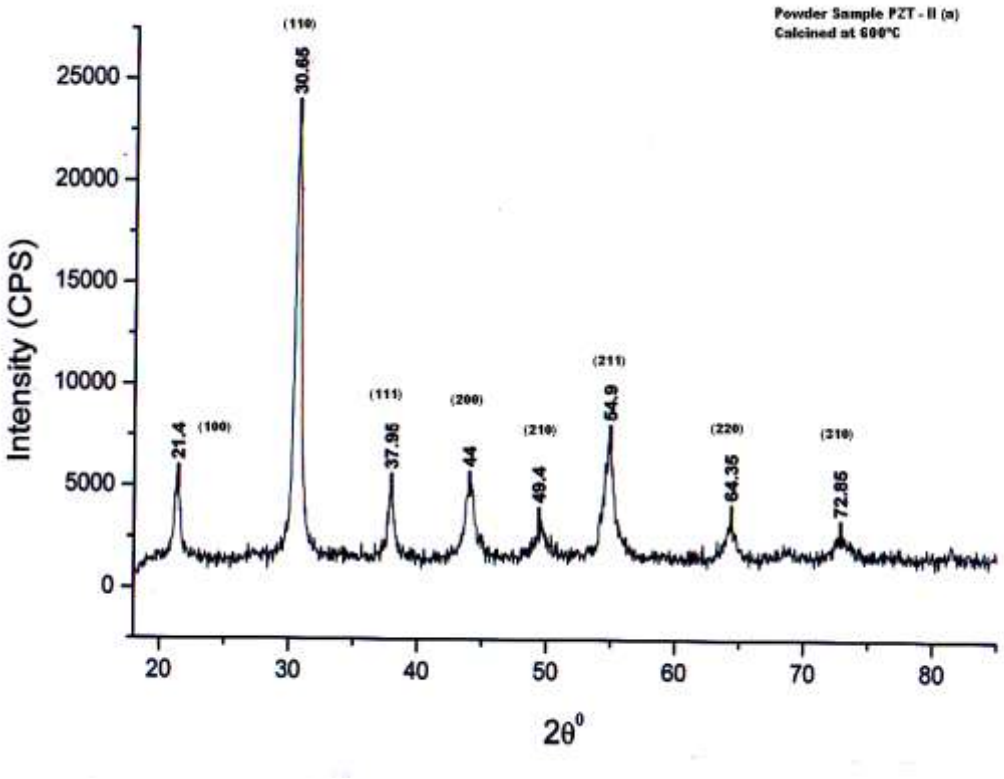

Fig. 6.4: *XRD Pattern of PZT – II Powder Calcined at 600^{o}C*

PZT – II XRD pattern substantiate that, at 600^{o}C a single phase perovskite structure obtained on different lattice planes as identified by XRD pattern in form of respective peaks at 2theta angle 21.4^{o}, 30.65^{o}, 37.95^{o}, 44^{o} and 49.4^{o}, 54.9^{o}, 64.35^{o}, 72.85^{o} against lattice planes (100), (110), (111), (200), (210), (211), (220) and (310) respectively. In addition, the intensity of peaks obtained in case of calcined powder was five times stronger then the powder dried at 300^{o}C. This observation showed that the PZT perovskite phase obtained at 600^{o}C was better crystallized.

The PZT powder's average crystallite size was calculated to be approximately *28 ± 5.3 nm* by using Scherrer's equation [51],

$$t = 0.9\,\lambda / B \cos \Theta_B \quad \ldots\ldots\ldots\ldots \quad \text{(Eq. 6.5)}$$

Where t is the average crystallite size in angstroms, B is the full width at half maximum (FWHM) in radians, λ is the wavelength in angstroms, and Θ_B is the Bragg angle in radians.

The SEM micrographs of powder samples PZT – I dried at 300^oC & PZT – II calcined at 600^oC are shown in fig. 6.5 & 6.6.

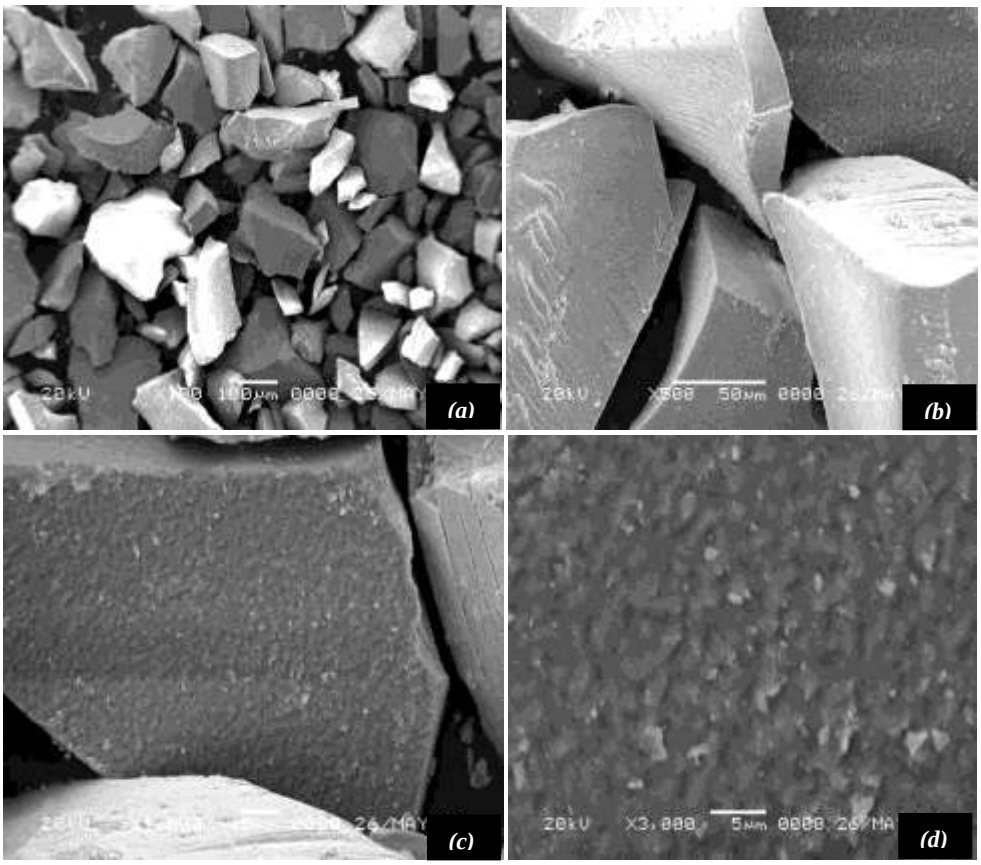

Fig. 6.5: *SEM images of PZT – I powder dried at 300^oC*

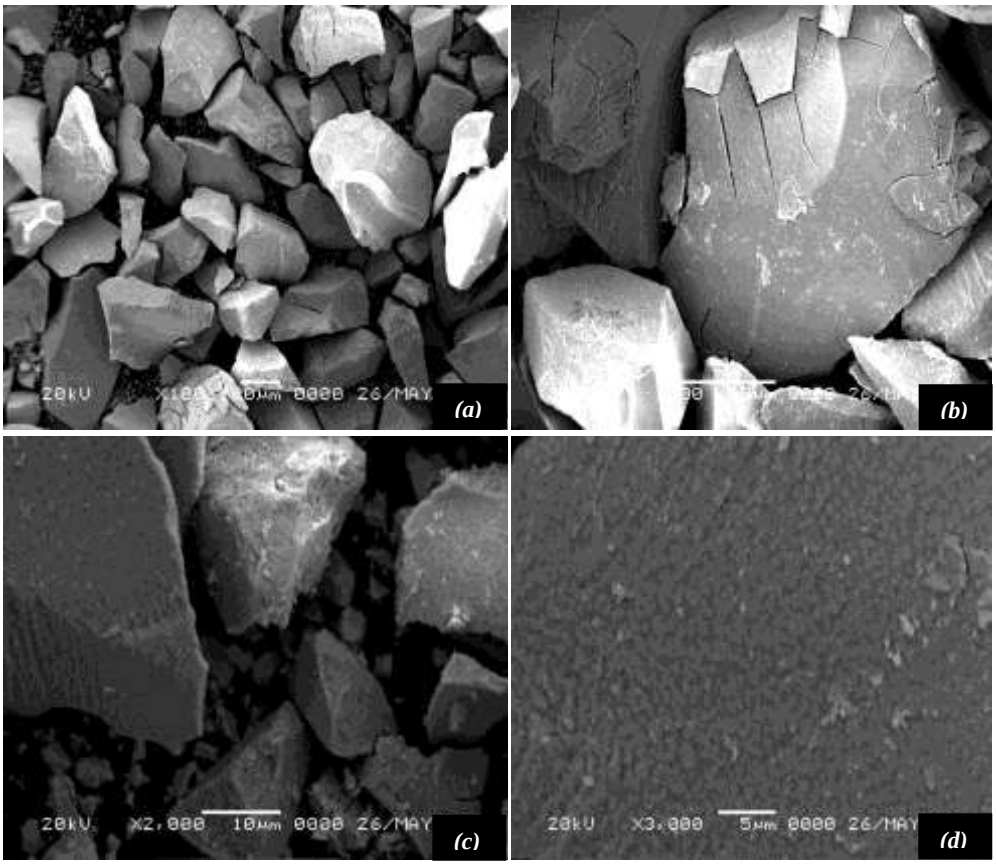

Fig. 6.6: *SEM images of PZT – II powder calcined at 600^{o}C*

In Figure 6.5 (a & b) SEM micrograph of grounded PZT – I powder at magnification x100 showed sharp edges of powder particles lumps indicated the brittle nature of powder particle lumps. The powder calcined at 600^{o}C showed prominent cracks with in the powder particle lumps (6.6 b), though no such cracks were observed in powder dried at 300^{o}C, indicated that with the increase in temperature shrinkage with in the powder particle lumps occur due to evaporation of low volatile materials and decomposition of organic species. Due to such shrinkage, cracks produced with in the powder particle lumps. These cracks propagate with in the powder particle lumps and resulted separation of some fine powder agglomerates at sharp edges as shown in fig. 6.6 (c).

At magnification x3000 (Fig 6.5d & 6.6d), within the powder particle lumps, clusters of fine agglomerates were shown. Powder calcined at 600^{o}C showed

significant agglomerates refinement then the powder obtains at 300^{o}C; indicate that with in powder particle lumps, agglomerates size decrease.

Thus in light of above, it can be suggested that with the increase in temperature from 300^{o}C to 600^{o}C, a prominent self accelerated decrease in powder particle size occurred due to decomposition and evaporation of organic species.

6.2 **Sol-Gel Dip Coated Samples:**

Four samples of PZT thin film were prepared through sol-gel dip coating process, on two substrates, silicon and brass (70:30). First of all, substrates were dipped in sol and allowed to form a wet film on their surface. After the film formation, the same was subjected to a heat treatment process for removal of residual organic species (entrapped solvent as well as the organic constituents associated with the precursor species), densification (elimination of residual porosity and structural free volume in the film), and crystallization.

The organic removal step was carried out 300^{o}C in an oven and calcination was carried out in muffle furnace at 600^{o}C. As solvent is removed from the film fine - scale (nm size) porosity may be created. At the interface with the solvent remaining in the pores, significant pressures can develop. These pressures contribute to capillary contraction, which can be a substantial driving force for the structural collapse of the film, which leads to densification. As the film collapses, reactive groups on different precursor molecules within the film come into closer proximity, which causes additional condensation reactions.

This densification mechanism accelerated as temperature increases and organic groups from the precursor species were removed. Once the bulk of the organic materials have been removed from the film, other characteristics of the film will be altered, including the structural free volume associated with the inorganic amorphous state [42]. This “structural relaxation” leads to continued densification of the film. This mechanism was significantly verified by SEM & AFM analysis

The SEM micrographs of PZT single layer thin film coated on silicon substrates are shown in fig 6.7.

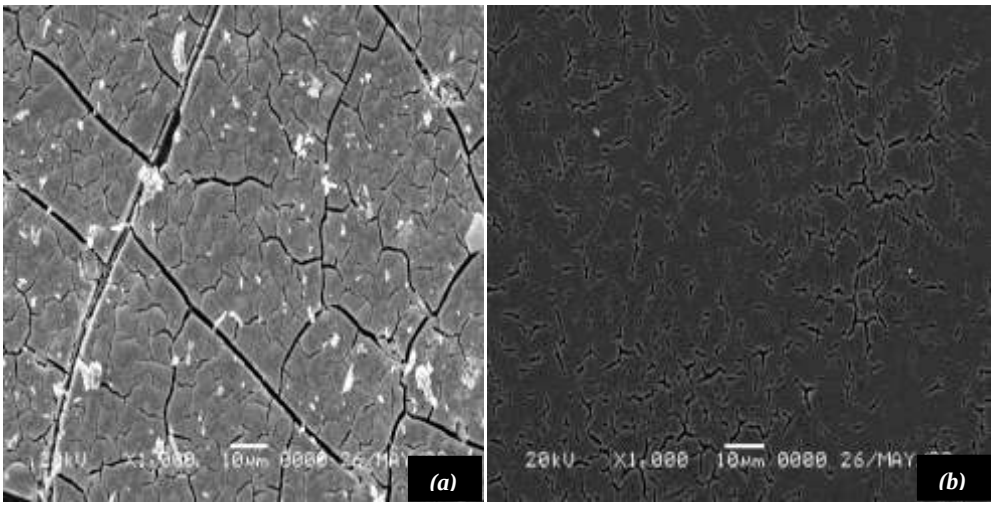

Fig. 6.7: *SEM micrograph of PZT thin films on silicon substrates*
(a) *at 300^{o}C* **(b)** *at 600^{o}C*

In fig. 6.7a, visibly large islands of coated layer were observed. The un-even line areas appeared in micrographs were due to evaporation of low volatile solvents that causes shrinkage with in the film. As the temperature is increased, the amorphous gel network is converted into crystalline form. The large islands start distributed uniformly that lead to increase in density of the thin film. The same thing was demonstrated by the SEM image of PZT thin layer single film obtained at 600^{o}C, fig. 6.7 (b). Hence at 600^{o}C a single phase and relatively dense perovskite structure were obtained.

The SEM micrographs of PZT single layer thin film obtained at 300^{o}C & 600^{o}C on brass (70:30) substrates (Fig. 6.8) showed similar sort of structures (Islands of PZT coated films) as observed in the case of PZT coating on silicon substrates.

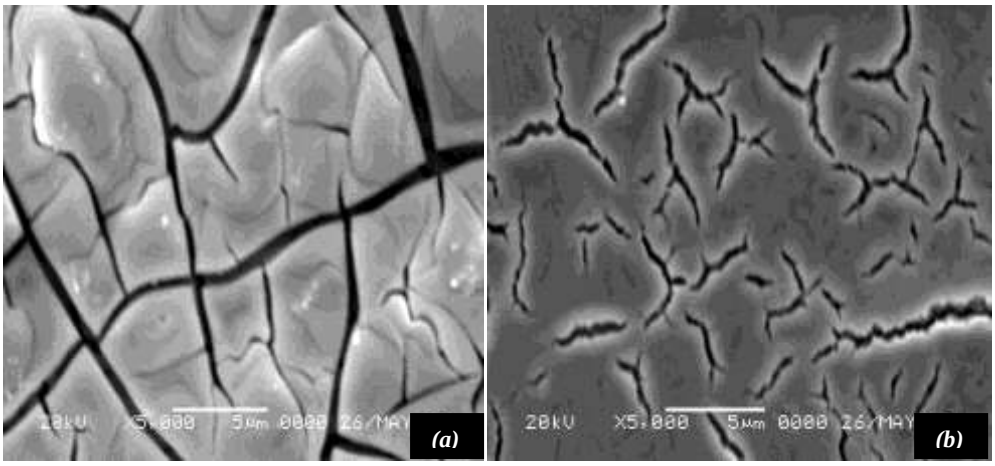

Fig. 6.8: *SEM micrograph of PZT thin films on brass (70:30) substrates*

(a) *at 300^{o}C* **(b)** *at 600^{o}C*

The Surface topography / morphology of PZT single and double layer thin film coated on silicon substrates were analyzed by using atomic force microscopy (fig. 6.9).

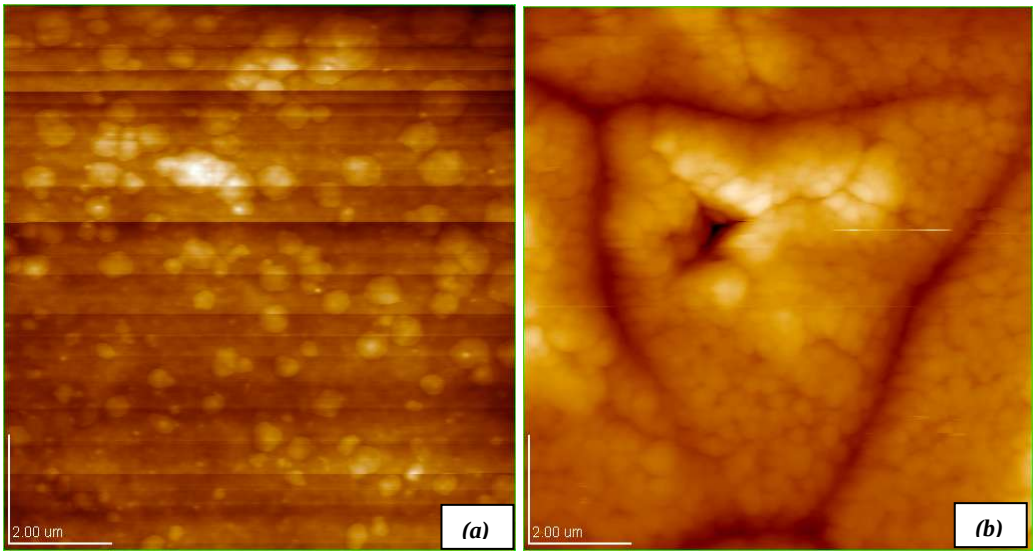

Fig. 6.9: *The AFM Image of PZT Thin Film calcined at 600^{o}C*

(a) *Single Layer* ***(b)*** *doubles Layer*

AFM images 6.9 (a) & (b) clearly showed that after first layer deposition, areas that remain un-coated due to evaporation of low volatile solvents were frequently filled by second layer coating. Hence, doubles layer deposited PZT thin film were more uniform & dense as compared to single layer PZT thin film.

A three dimensional view of PZT double layer thin film AFM image obtained at 600^{o}C shown in Figure 6.10. It can be seen that the PZT thin film obtained through sol gel dip coating process was of the order of nanometers. In present case, roughness of single & double layer PZT thin films up to 30nm and 78nm respectively were observed.

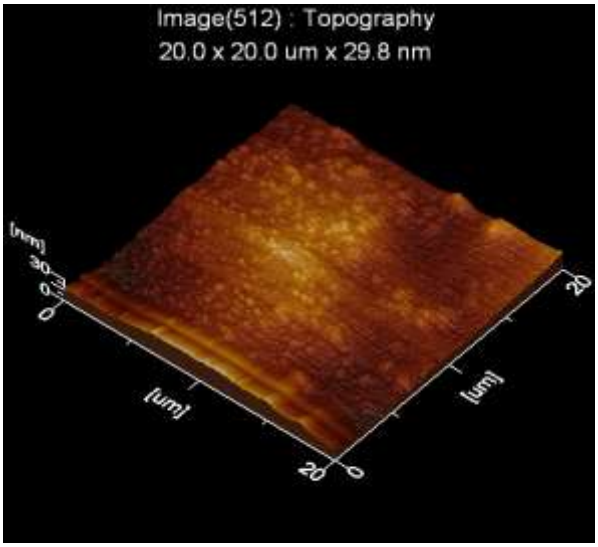

Fig. 6.10 (a): *The AFM 3D Image of PZT Thin Film treated at 600^{o}C (Single Layer)*

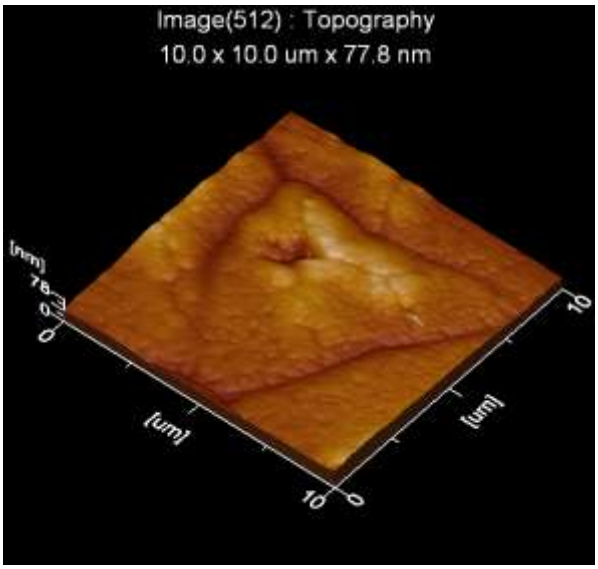

Fig. 6.10 (b): *The AFM 3D Image of PZT Thin Film treated at 600^{o}C (Double Layer)*

The SEM cross-section micrographs of PZT thin film on silicon substrate treated at 600^{o}C are shown in fig. 6.11.

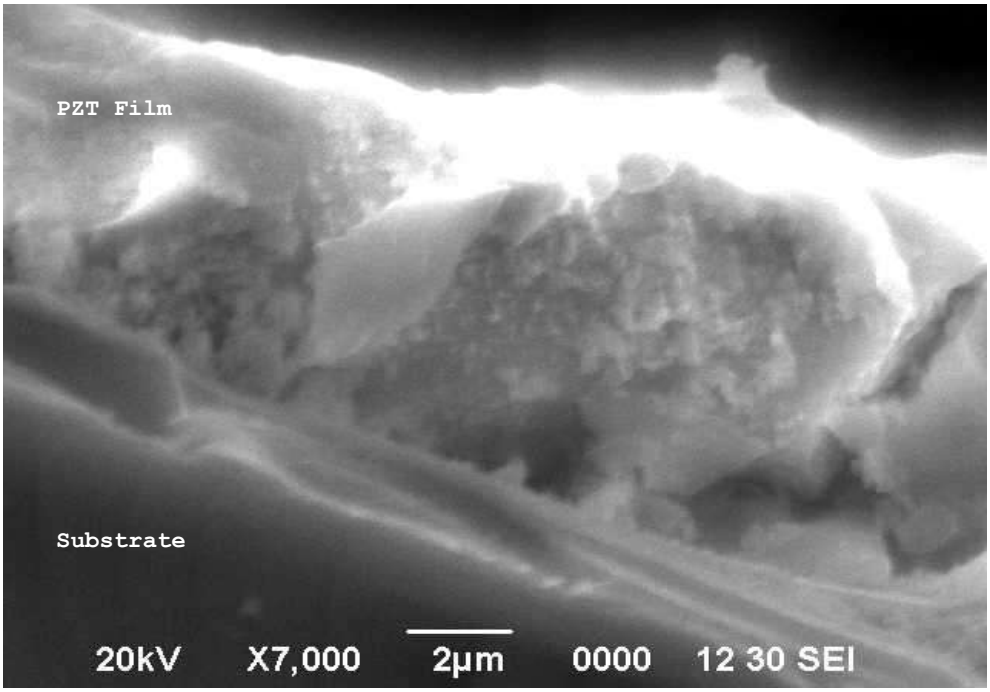

Fig. 6.11 (a): *SEM cross-section micrograph of PZT thin film on silicon substrates treated at 600^{o}C*

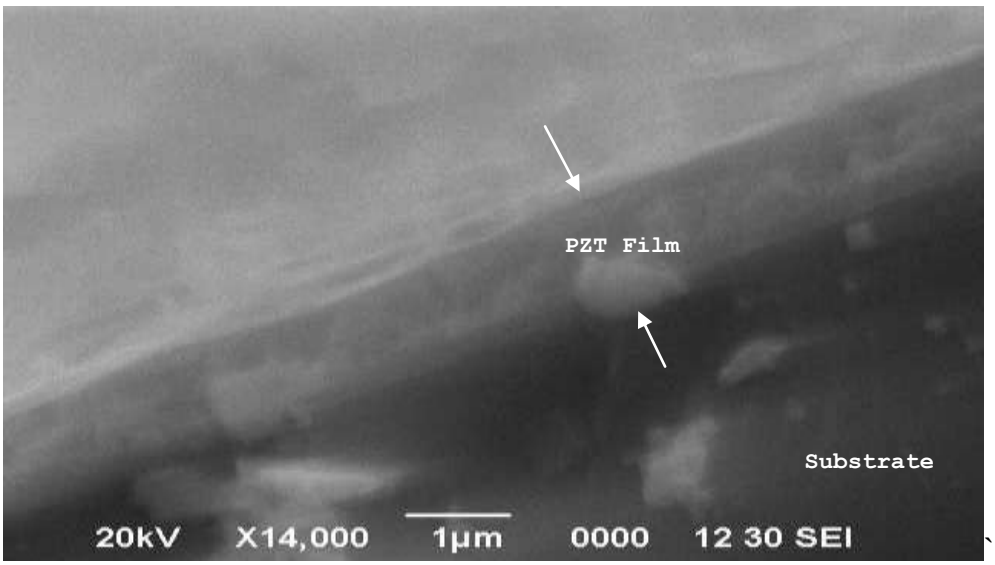

Fig. 6.11 (b): *SEM cross-section micrograph of PZT thin film on silicon substrates treated at 600^{o}C*

The SEM cross-section view of PZT thin films clearly indicate that a uniform and dense film was achieved with the thickness of ≈ 1μm. The particles seen in fig. 6.11 (b) were due to cutting / polishing of the cross-section of sample for SEM study.

Thus, in the light of SEM & AFM analysis, it can be concluded that a single phase, homogeneous and dense PZT thin films were successfully achieved through sol-gel dip coating technique.

6.3 ***Sol-Gel Spin Coated Sample:***

Sol-Gel dip coating process didn't require any complicated apparatus for coating the substrates. But in the case of sol-gel spin coating process, substrate had to rotate at constant speed and sol drops allowed to fall on the substrate very slowly. Due to centrifugal force, the drops spread over the substrate. Any excess sol in any area just spin off from the substrate surface and results a more uniform coating the sol-gel dip coating technique. Thus, keeping in view the basics of the spin coating process, the same technique was endeavored on self made arrangement at SCME, NUST for the first time and a thin, uniform PZT coating was successfully achieved.

The SEM micrographs of spin coated PZT thin film on brass 70:30 disc treated at 600^{o}C are shown in fig. 6.13.

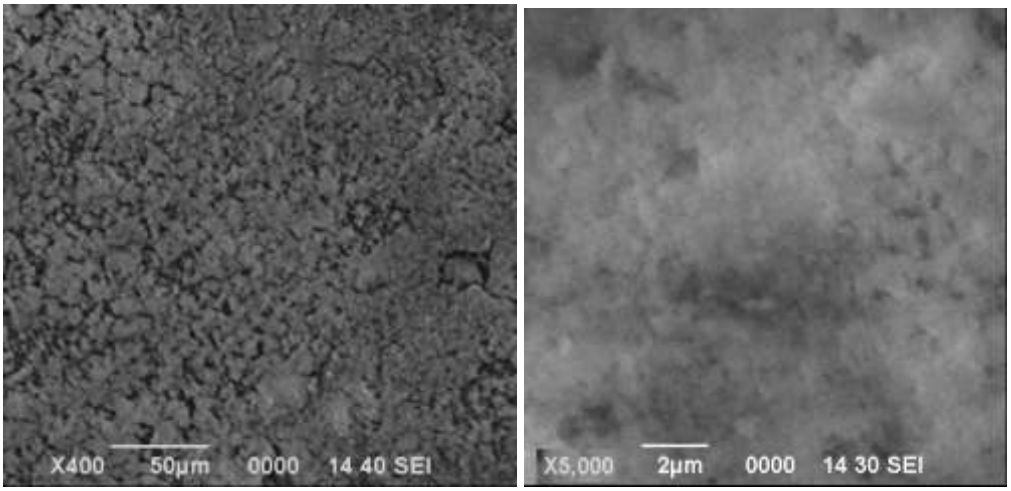

Fig. 6.12: *SEM micrographs of spin coated PZT thin film on Brass (70:30) disc treated at 600^{o}C*

SEM images (Fig. 6.12) demonstrate that a uniform spin coated PZT thin film was achieved. However, a considerable difference between dip coated and spin coated SEM microstructures were observed. In dip coated PZT thin films microstructure, islands with shrinkage lines were prominent but in case of spin coated PZT thin film, a uniform PZT film with micro-porosity were observed.

A possible reason in the difference of microstructure lies in the way the coating was achieved. During spin coating process, sol was introduced drop by drop (continuously) which spread from centre of disc to its periphery owing to centrifugal forces involved. Due to high speed rotation, the drying process started at coating stage. The sol started drying while the coating was still in progress. Dried areas were filled constantly due to continuous flow of sol from center to periphery. Hence, increase the population of PZT sol molecules on substrate. Where as no such back up sol fill up route involved in the case of dip coating process.

In the light of above discussion, it can be suggested that, the shrinkage lines observed in dip coated PZT thin film micro-structure and porosity in the case of spin coated PZT thin film microstructure was due to difference in way of filling the sol over the substrate surface. However, this finding need more work in future.

7

Conclusions

- ✓ Successfully prepared Lead Zirconate Titanate powder at 600^{o}C according to formula ***Pb (Zr $_{0.52}$ Ti $_{0.48}$)*** $\mathbf{O}_3$ through sol-gel processing, which was much lower PZT powder processing temperature as compared to conventional mixed oxide route i.e. 850^{o}C.

- ✓ In present study, acetic acid was used for preparation of the sol that creates the chelating effect. During hydrolysis, the acetate group of acetic acid bonds with the titanium atom and consequently prolongs the drying stage and hinders the gel formation.

- ✓ Successfully coated Lead Zirconate Titanate thin films on silicon and brass substrates through sol-gel dip coating process. The AFM & SEM analysis verified that the coated films were uniform and dense.

- ✓ In addition to sol-gel dip coating, the sol-gel spin coating process was also investigated for the first time at SCME, NUST on self made arrangement. The SEM analysis verified that a uniform PZT film was achieved on brass (70:30) disc.

- ✓ The shrinkage lines observed in dip coated PZT thin film micro-structure and porosity in the case of spin coated PZT thin film microstructure was due to difference in way of filling the sol over the substrate surface.

8

Future Suggestions

- ✓ By introducing seeding concept PZT powder and thin film can be obtained at much lower temperature then 600^{o}C.
- ✓ Measurements of Piezoelectric properties of PZT powder & thin films.
- ✓ Study of the affect of ageing on piezoelectric properties of PZT thin films.
- ✓ Study of affect of dopants on piezoelectric properties of PZT powder & thin films.
- ✓ Factors affecting the Spin & Dip coated PZT thin films microstructure.

Reference:

[1] *F. Smith, Foundations of Materials Science and Engineering, 3rd Edition, The McGraw-Hill Companies, 8-9, (2004)*

[2] *C. Barry Carter, M. Grant Norton, Ceramic Materials Science and Engineering, The Springer Inc, (2007).*

[3] *M. Khalid, "Processing and Ferroelectric Properties of $Pb_{0.91}Sr_{0.09}(Zr_{0.53}Ti_{0.47})O_3$ Ceramics" MS Thesis, Department of Material Engineering. School of Chemical & Material Engg. (SCME), NUST, (2008).*

[4] *H. Zheng, I. M. Reaney, W. E. Lee, N. Jones and H. Thomas "Surface Decomposition of Strontium-Doped Soft $PbZrO_3$–$PbTiO_3$" J. Am. Ceram. Soc., 85 [1] 207–12 (2002).*

[5] *A. I. Kingon and J. B. Clark, "Sintering of PZT ceramics: II, "Effect of PbO content on densification kinetics". J. Am. Ceram. Soc., Vol 66 No.4 256-260 (1983).*

[6] *A. I. Kingon and J. B. Clark, "Sintering of PZT ceramics: I, "Atmosphere Control". J. Am. Ceram. Soc., Vol 66 No.4 (1983) 253-256.*

[7] *B. Malic and M. Kosec, "Electron Microscope Study of Alkoxide-Derived Compositions within the PbZrO3–PbTiO3 Phase Diagram," J. Sol–Gel Sci. Technol., 2, 443–46 (1994).*

[8] *M. Villegas, C. Moure, J. R. Jurado, and P. Duran, "Processing and Properties of Pb(Mg1/3Nb2/3)O3–PbZrO3–PbTiO3 Ceramic Relaxors," J. Mater. Sci., 29, 4975–83 (1994)*

[9] *C. T. Lin, B. W. Scanlan, J. D. McNeill, J. S. Webb, L. Li, R. A. Lipeles, P. M. Adams, and M. S. Leung, "Crystallization Behavior in a Low-Temperature Acetate Process for Perovskite PbTiO3, Pb(Zr,Ti)O3, and (Pb1–x,Lax)(Zry,Ti1–y)1–x/4O3 bulk Powders," J. Mater. Res., 7, 2546–54 (1992).*

[10] *J. Chen, M. P. Harmer, and D. M. Smyth, "Compositional Control of Ferroelectric Fatigue in Perovskite Ferroelectric Ceramics and Thin Films," J. Appl. Phys., 76 5394–98 (1994).*

[11] *K. Kakegawa, O. Matsunaga, T. Kato, and Y. Sasaki, "Compositional Change and Compositional Fluctuation in Pb(Zr,Ti)O3-Containing Excess PbO," J. Am. Ceram. Soc., 78 1071–75 (1995).*

[12] *R.C. Asher, Ultrasonic Sensors For Chemical & Process Plant, 84-87, (1997).*

[13] *T. Wolfram, Electronic and Optical Properties of D-Band Perovskites, Middle East Technical University, Ankara, 1-3 (2006).*

[14] *T.L. Jordan, Z.Ounaies Piezoelectric Ceramics Characterization NASA / CR-2001-211225 ICASE Report No. 2001-28, September (2001).*

[15] *W.D. Kingery, Y.M. Chiang, D. Birinie, Physical Principles of Ceramic Science & Engineering, MIT Series in Materials and Engineering, John Wiley and Sons, Inc. USA, (1997).*

[16] *S. Zahi, R. Bouaziz, N. Abdessalem, A. Boutarfaia, Ceramic Introduction 29, 35–39 (2003).*

[17] *S. Zhao, H. Wu, Q. Sun, Materials Science and Engineering B, 123, 203–210 (2005).*

[18] *K. Nagashima, M. Aratani, and H. Funakubo, J. Appl. Phys., 89, 4517 (2001).*

[19] *B. Jaffe, W. R. Cook Jr., and H. Jaffe, Piezoelectric Ceramics (Academic Press, London, 1971).*

[20] *N. Tohge, S. Takahashi, and T. Minami, J. Am. Ceram. Soc., 74, 67 (1991).*

[21] *R. C. Buchanan, ed., Ceramic Materials for Electronics - Processing, Properties and Applications (Marcel Dekker, New York, 1986.*

[22] *C.J. Brinker and G.W. Scherer, Sol-gel science — the physics and chemistry of sol-gel processing, Academic Press, 1990*

[23] *W. Geffcken and E. Berger, Verfahren zur A¨nderung des Reflexionsvermo¨gens optischer Gl¨aser, German Patent 736 411 (1943)*

[24] *H. Dislich and P. Hinz, "History and principles of the sol-gel process, and some new multicomponent oxide coatings", J. Non-Cryst. Solids, 48:11–16 (1982)*

[25] *B. Yoldas, "Preparation of glasses and ceramics from metal-organic compounds", Journal of Material Science, 12:1203–1208 (1977)*

[26] *Fukushima , J. ; Kodaira , K. ; Matsushita , T. Preparation of ferroelectric PZT films by thermal decomposition of organo-metallic compounds. J. Mat. Sci. 19: 595 – 598 (1984).*

[27] *Dey , S. K. ; Budd , K. D. ; Payne , D. A. Thin - film ferroelectrics of PZT by sol - gel processing. IEEE Trans. UFFC. 35: 80 – 81 (1988).*

[28] *Brinker, C. J.; Scherer, G. W. Relationships between the sol - to - gel and gel - to - glass conversions . In Ultra-structure Processing of Ceramics, Glasses, and Composites, edited by Hench , L. L. ; Ulrich , D. R. John Wiley & Sons, Inc. , New York .43 – 59 (1984).*

[29] *Schwartz , R. W. ; Lakeman , C. D. E. ; Payne , D . A. The effects of hydrolysis conditions, and acid and base additions, on the gel - to - ceramic conversion in sol - gel derived $PbTiO_3$. In Better Ceramics Through Chemistry IV , edited by Zelinski , B. J. J. ; Brinker , C. J. ; Clark , D. E. ; Ulrich , D. R. Mat. Res. Soc. Symp. Proc. 180 : 335 – 340 (1990) .*

[30] *Schwartz, R. W.; Payne, D. A.; Holland, A. J. The effects of hydrolysis and catalysis conditions on the surface area and decomposition behavior of polymeric sol - gel derived $PbTiO_3$ powders. In Ceramic Powder Processing Science, edited by Hausner , H . ; Messing , G . W. ; Hirano , S. Deutsche Keramische Gesellschaft. pp. 165 – 172 (1989).*

[31] *Scriven, L. E. In Better Ceramics through Chemistry III; Materials Research Society: Pittsburg, PA,, pp. 717–729 (1988).*

[32] *Brinker , C. J. ; Hurd , A. J. Fundamentals of sol - gel dip – coating J. Phys. III France. 4 : 1231 – 1242 (1994).*

[33] *Schwartz, R. W. ; Schneller , T. ; Waser , R. Chemical solution deposition of electronic oxide thin fi lms . C R Chemie 7 : 433 – 461(2004).*

[34] *Scriven , L. E. Physics and applications of dip coating and spin coating. In Better Ceramics Through Chemistry III , edited by Brinker , C. J. ; Clark , D. E. ; Ulrich , D. R. Mat. Res. Soc. Symp. Proc. 121: 717 – 729 (1988).*

[35] *Scriven , L. E . Physics and applications of dip coating and spin coating. In Better Ceramics Through Chemistry III , edited by Brinker , C. J. ; Clark , D. E. ; Ulrich , D. R. Mat. Res. Soc. Symp. Proc. 121: 717 – 729 (1988).*

[36] *Licari , J. J. Coating Materials for Electronic Applications: Polymers, Processes, Reliability, Testing. Noyes Publications, William Andrew Publishing, New York (2003).*

[37] *Tuttle, B. A.; Schwartz, R. W. Solution deposition of ferroelectric thin films .Mat. Res. Bull. 21: 49 – 54 (1996).*

[38] *Brennecka , G. ; Tuttle , B. Deposition of ultra thin film capacitors fabricated by chemical solution deposition. J. Mat. Res. 22: 2868 – 2874 (2007).*

[39] *Lu, Y. T.; Milne, S. J. Processing and characterization of $Pb(Zr,Ti)O_3$ films, up to 10u□m thick, produced from a diol sol - gel route . J. Mat. Res. 11: 2556 – 2564 (1996).*

[40] *Lu, Y. T.; Calzada, M. L.; Phillips, N. J.; Milne, S. J. Synthesis and electrical characterization of thin films of PT and PZT made from a diol based sol - gel route .J. Am. Ceram. Soc. 79: 441 – 448 (1996).*

[41] *Phillips, N. J.; Calzada , M. L. ; Milne , S. J. Sol - gel - derived lead titanate films . J. Non - Cryst. Sol. 147 / 148: 285 – 290 (1992).*

[42] *Schwartz , R. W. ; Lakeman , C. D. E. ; Payne , D. A. The effects of hydrolysis conditions, and acid and base additions, on the gel - to - ceramic conversion in sol - gel derived $PbTiO_3$. In Better Ceramics Through*

Chemistry IV , edited by Zelinski , B. J. J. ; Brinker , C. J. ; Clark , D. E. ; Ulrich , D. R. Mat. Res. Soc. Symp. Proc. 180: 335 – 340 (1990).

[43] *Schwartz , R. W. ; Payne , D. A. Crystallization behavior of chemically prepared and rapidly solidified $PbTiO_3$. In Better Ceramics Through Chemistry III , edited by Brinker , C. J. ; Clark , D. E. ; Ulrich , D. R. Mat. Res. Soc. Symp. Proc. 121: 199 – 206 (1988).*

[44] *Tuttle , B. A. ; Voigt , J. A. ; Headley , T. J. ; Potter , Jr. , B. G. ; Dimos , D. ; Schwartz , R. W. ; Dugger , M. T. ; Michael , J. ; Nasby , R. D. ; Garino , T. J. ; Goodnow , D. C. Ferroelectric thin fi lm microstructure development and related property enhancement. Ferro. 151 (1 – 4): 11 – 20 (1994).*

[45] *Waser , R. ; Schneller , T. ; Hoffmann - Eifert , S. ; Ehrhart , P . Advanced chemical deposition techniques from research to production. Int. Ferro. 36: 3 – 20 (2001).*

[46] *Waser , R. ; Schneller , T. ; Ehrhart , P. ; Hoffmann - Eifert , P. Chemical deposition methods for ferroelectric thin fi lms . Ferro. 259 (1 – 4): 205 – 214(2001) .*

[47] *Dobberstein , H. ; Schwartz , R. W. Modeling the nucleation and growth behavior of solution derived thin films . Proc. 1 st Symp. Adv. Mat. Next Generation —Prelude to Func. - Int. Mat. (AIST Chubu , Nagoya, Japan) (2002).*

[48] *Hyun Tae Lee, Wan In Lee, Yoo Hang Kim, and Chin Myung Whang, "The Seeding Effects on the Phase Transformation of Sol-Gel Derived PZT Powder" Bull. Korean Chem. Soc. Vol. 23, No. 8, 1078 – 1084 (2002).*

[49] *W. D. Yang, ''PZT/PLZT Ceramics Prepared by Hydrolysis and Condensation of Acetate Precursors,'' Ceram. Inter., 27, 373–84 (2001).*

[50] *R. Merkle and H. Bertagnolli, ''Investigation of the Pyrolysis of Lead Zirconate Titanate Gels with Coupled Differential Thermal Analysis, Thermo-gravimetry and Infrared Spectroscopy,'' J. Mater. Sci., 33, 4341–8 (1998).*

[51] *B.D. Cullity and S.R. Stock, Elements of X-Ray Diffraction, 3rd Edition, Prentice – Hall, Inc. New Jersey, USA, (2000).*